Analysis of Non-isothermal Adsorption of Carbon dioxide in Metal Organic Frameworks

by

John Nkuutu

A Thesis Presented in Partial Fulfillment
of the Requirements for the Degree
Master of Science

Approved April 2023 by the
Graduate Supervisory Committee:

Jerry Lin, Chair
Heather Emady
Shuguang Deng

ARIZONA STATE UNIVERSITY

May 2023

ABSTRACT

Adsorption is fundamentally known to be a non-isothermal process; in which temperature increase is largely significant, causing fairly appreciable impacts on the process kinetics. For porous adsorbent particles like metal organic frameworks (MOFs), silica gel, and zeolite, the resultant relative heat generated is partly distributed within the particle, and the rest is transferred to the surrounding ambient fluid (air).

For large step changes in adsorbed phase concentration and fast adsorption rates, especially, the isothermality of adsorption (as in some studies) is an inadequate assumption and inspires rather erroneous diffusivities of porous adsorbents. Isothermal models, in consequence, are insufficient for studying adsorption in porous adsorbents. Non-isothermal models can satisfactorily and exhaustively describe adsorption in porous adsorbents. However, in many of the analyses done using the models, the thermal conductivity of the adsorbent is assumed to be infinite; thus, particle temperature is taken to be fairly uniform during the process—a trend not observed for carbon dioxide (CO_2) adsorption on MOFs.

A new and detailed analysis of CO_2 adsorption in a single microporous MOF-5 particle, assuming a finite effective thermal conductivity along with comprehensive parametric studies for the models, is presented herein. A significant average temperature increase of 5K was calculated using the new model, compared to the 0.7K obtained using the Stremming model. A corresponding increase in diffusivity from 8.17×10^{-13} to 1.72×10^{-11} m^2/s was observed, indicating the limitations of both isothermal models and models that assume constant diffusivity.

ACKNOWLEDGEMENT

I would like to express my deepest appreciation to Dr. Jerry Lin for the chance he offered me to work with him on this project. The continued support, help, and guidance I have received from him over the time I have worked on this research were key to its successful completion. I would not have been able to reach this point without his invaluable insights and dissections into the topic.

In the same manner, I wish to extend my sincere appreciation to Dr. Heather Emady and Dr. Shuguang Deng for gladly accepting to serve on my thesis committee. The support and knowledge I received from them, as well as the courses they taught me, have been instrumental towards the successful completion of this thesis.

My family and friends, from whom I have been distant against my will, have continuously provided immense encouragement and support throughout the process.

I am indebted to all of you!

TABLE OF CONTENTS

CHAPTER Page

APPENDIX **Page**

LIST OF TABLES

LIST OF FIGURES

Figure **Page**

Figure **Page**

Chapter 1

INTRODUCTION

Adsorption in its simplest literal meaning refers to the transfer of fluid molecules (called the adsorbate) onto a solid surface (also known as the adsorbent) as a result of unbalanced forces. This mass transfer is enabled by the adsorbent's ability to preferentially attract and concentrate liquid or gaseous molecules on their surfaces.[24] It is an exothermic process during which considerable amounts of heat are given out to the surrounding. Desorption, on the other hand, is the movement of adsorbate species from the solid surface to the bulk of gas of liquid.

Adsorption is categorized into two major categories; chemical or physical– depending on how the adsorbate and adsorbent interact with each other. Physical adsorption (or physiosorption) occurs due to the weak Van der Waals forces with which the adsorbent interacts with the adsorbate.[2] It is a reversible process that usually occurs at relatively lower temperatures, and the corresponding heat of adsorption is low. Chemical adsorption (also known as chemisorption) results from the formation of chemical covalent bonding between adsorbate molecules and the adsorbent active sites, and it occurs at various temperatures.[1] The resultant heat of adsorption for this type of adsorption is comparatively higher. Table 1.1 below summarizes the differences between chemical and physical adsorptions. Electrostatic adsorption (also known as ion exchange) is another form of adsorption which entails the coulombic attractive forces between ions and charge functional groups.[9] This ion-ion interaction takes advantage of the variance in ionic valencies and diameters to carry out selective adsorption of ions, and usually applied in the construction of electrodes, ion exchange filters among others.

The process of adsorption occurs in many biological and physical systems, and it is a widely used technique in various industrial applications. An adsorbate is contacted with the adsorbent placed in an adsorption column or tank where the process occurs.

Table 1.1: Differences between chemical and physical adsorptions

Chemical Adsorption	Physical Adsorption
High heat of adsorption	Low heat of adsorption
Highly specific[19]	Non-specific[19]
Slow and irreversible	Rapid and reversible
Mono-layer[19]	Can be mono- or multi-layer[19]
Dissociative[19]	non-dissociative[19]
Significant over different temperatures[9]	Below gas' condensation point [9]

For instance, during water purification, alum stone is added to the impure water so that impurities organic pollutants can get adsorbed on the alum.[2] Silica gel also is used to remove moisture from wet air. To accomplish this, an adsorption column is filled with a suitable hydrophilic adsorbent that removes traces of moisture from the air to be dried.

1.1 Adsorption Diffusion

Adsorption process is based on the extent of the diffusional resistances associated with the mass transfer of diffusing molecules from the bulk fluid, through the substrate's pores, to the pore surfaces as shown in figure 1.1 below; as well as the adsorption reaction rate (for the case of chemisorption). Thus, adsorption is sometimes

considered an equilibrium-diffusion reaction process.[24] Intracrystalline micropore diffusion, external fluid film diffusion and macropore diffusion are some of the significant resistances during the process. Depending on the nature of the adsorbent, the rate of adsorption and desorption is driven by one or a combination of these resistances.

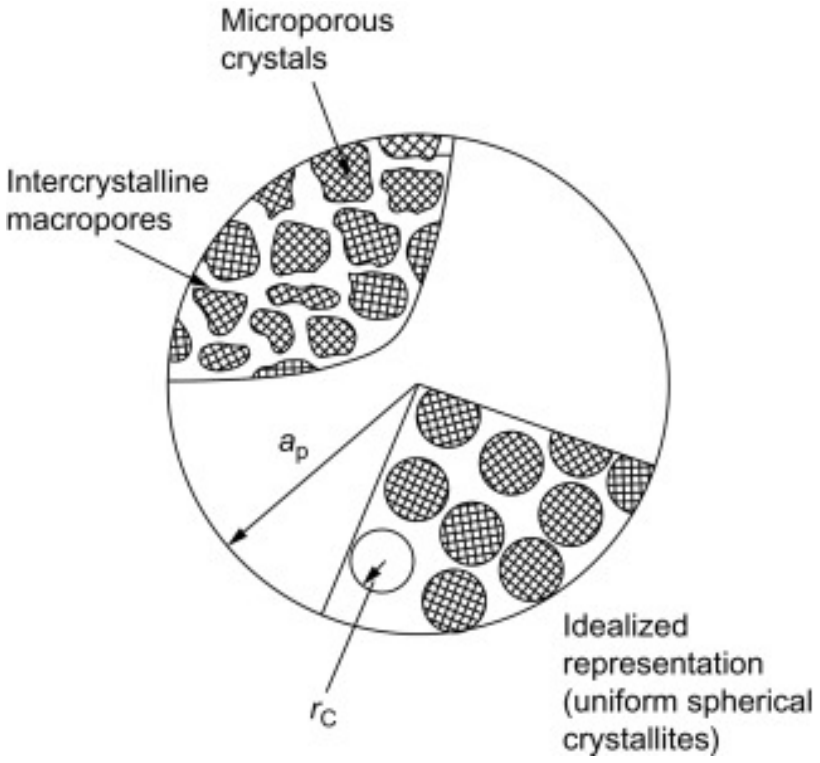

Figure 1.1: Schematic representation of the mass transfer resistances for an adsorbent pellet [Adapted from: Ruthven [19]]

1.1.1 Diffusion in Porous Compounds

Generally, diffusion in porous materials is governed by; (1) mass transfer from the bulk fluid to the external surface of the adsorbent, and (2) intrapellet diffusion.[19] When a gas is introduced around an adsorbent particle, its partial pressure relative to the atmospheric pressure around the particle increases, facilitating surface diffusion

of its molecules onto the solid, and subsequently into the pores.

Porosity of the adsorbent is an important parameter in determining how much of adsorptive molecules around the adsorbent particle is transferred through the particle pores.[9] The property is attributed to adsorbent's structure, and it depends on how the solid is synthesized and treated. It is determined by both bulk particles and the "detachment of a part of the mass of the solid."[9] The bigger the porosity, the easier it is for sorbate molecules to diffuse through pores and vice versa. For micro intracrystalline pores, surface diffusion occurs where sorbate mass transfer takes place due to an activated process that involves movement at sorption sites. Diffusion in larger pores in which the diffusing sorbate particle can escape from the surface field is termed as macropore diffusion.

Adsorption in porous materials is driven by the sorbate mass transport within the pore network, rather than the surface sorption kinetics[19], and is dependent on both pore size as well as sorbate concentration. There is usually less bulk sorbate transport through the pore system, thus intraparticle sorbate transport can be considered a diffusive process described by the Fickian diffusion as shown in equation 1.1 below:

$$J = -D(c)\frac{\partial c}{\partial x} \tag{1.1}$$

where D is diffusivity, c is fluid concentration, x is a coordinate, and J is the flux of mass diffusion. The true driving force of any mass transport (diffusion in this case), however, is the chemical potential gradient, and not sorbate concentration gradient.[19] Yet, in the above expression, the implication is that diffusivity is not dependent on the concentration gradient.

A new parameter called mobility, B(c), is introduced in equation (1.1) to relate mass

diffusion flux and chemical potential gradient as shown:

$$J = -Bc\frac{\partial \mu}{\partial x} \tag{1.2}$$

Considering a sorption process involving an ideal vapor phase at equilibrium, the vapor can be taken to be an ideal gas, and chemical potential can be defined as:

$$\mu = \mu^0 + RT \ln a = \mu^0 + RT \ln p \tag{1.3}$$

$$\frac{\partial \mu}{\partial x} = RT\frac{\partial \ln a}{\partial x} = RT\frac{d \ln p}{dc}\frac{\partial c}{\partial x} \tag{1.4}$$

Implying,

$$J = -BRTc\frac{d \ln p}{dc}\frac{\partial c}{\partial x} = -BRT\frac{d \ln p}{d \ln c}\frac{\partial c}{\partial x} \tag{1.5}$$

Comparing equations 1.1 and 1.5, it is seen that Fickian diffusivity is defined as:

$$D = BRT\frac{dl \ln p}{d \ln c} = D_0\frac{d \ln p}{d \ln c} \tag{1.6}$$

in which dln(p)/dln(c) is the slope of the equilibrium isotherm. $D_0 = BRT$ is the corrected diffusivity. The corrected diffusivity expression is sometimes called the Darken equation because it was used by Darken in 1946,[22] despite being suggested earlier by Maxwell.[14] D_0 is not necessarily independent of concentration although it is the case in many experimental evidence for a number of systems.[10]

1.2 Adsorption Kinetics

It is of essence to understand adsorption kinetics because they describe the rate of adsorption, r_{ads}, onto the adsorbent solid surface. The rate may be expressed in terms of fluid partial pressure around the particle as shown in equation 1.7 below

$$r_{ads} = kp^n \tag{1.7}$$

in which n is the kinetic order, k is the rate constant, and p is the fluid partial pressure. In the Arrhenius form, the expression becomes equation 1.8, in which A is the pre-exponential factor, and E_a is the activation energy, which is the energy required to overcome the chemical bond formation between the adsorbate molecules and the solid surface, R is the gas constant, whereas T is the ambient temperature of the fluid gas.

$$r_{ads} = Ae^{-E_a/RT}p^n \tag{1.8}$$

Since rate of adsorption is determined by rate of transfer of adsorbate molecules as well as the proportion of incident molecules onto the adsorbent surface, it is sufficient to express r_{ads} in terms of molecular flux, J, and sticking probability, s_0[16], as well as in terms of the number of adsorbed species per unit area of surface, N_{ads}, and time, t, i.e.,

$$r_{ads} = Js_0 = \frac{dN_{ads}}{dt} \tag{1.9}$$

The sticking probability is the likelihood of adsorbate particles to get adsorbed onto the adsorbent whose value ranges from 0 to 1. It is dependent on the existing coverage of adsorbed species and the activation barrier to adsorption, while the molecular flux, J can be described using Hertz-Knudsen equation:

$$J = \frac{p}{\sqrt{2\pi m k_B T}} \tag{1.10}$$

where m is the fluid molecular mass and k_B is the the Boltzmann constant. The sticking probability, s_0 is expressed by:

$$s_0 = f(\Theta)e^{-E_a/RT} \tag{1.11}$$

where Θ is the coverage. Combining equations (1.10) and (1.11), the general expression for the rate of physical and chemical adsorptions becomes:

$$r_{ads} = \frac{f(\Theta)p}{\sqrt{2\pi m k_B T}}e^{-E_a/RT} \tag{1.12}$$

From equations (1.7) and (1.12), it is sufficient to conclude the rate of adsorption is expected to be first order with respect to the partial pressure of the gas around the adsorbent particle. The expression in equation (1.12) describes rates of both physical and chemical adsorptions —depending on the value approximations of $f(\Theta)$; for instance when $f(\Theta) = (1\text{-}\Theta)$, the process is first order and valid for physical adsorption[5] while for $f(\Theta) = (1\text{-}\Theta)^n$, then adsorption is valid for "dissociative" chemical adsorption, where n is the order of chemisorption.

Integration of equation (1.9) gives

$$N_{ads} = Js_0t \tag{1.13}$$

which gives the number of adsorbed species per unit area of the adsorbent surface.

1.3 Adsorption Thermodynamics

Thermodynamics parameters indicate whether or not the adsorption process is spontaneous. For a negative enthalpy value of an adsorption process, the Gibb's free energy is negative, making the adsorption process spontaneous. In addition to the Gibb's free energy and enthalpy, entropy is another thermodynamic parameter that contributes to the spontaneity and feasibility of adsorption. The three parameters are related by the following expression:

$$\Delta G^o = \Delta H^o - T\Delta S^o \tag{1.14}$$

T in the equation is temperature which affects the kinetic energy of gas particles, influencing the diffusion of these molecules, and consequently shifting the adsorption equilibrium position. At a given temperature, ΔG^o is given by Van't Hoff equation[13] as shown below:

$$\Delta G^o = -RT \ln K_e \tag{1.15}$$

in which K_e is a dimensionless thermodynamic equilibrium constant. Equations (1.14) and (1.15) give the following expression:

$$\ln K_e = -\frac{\Delta H^o}{RT} + \frac{\Delta S^o}{R} \tag{1.16}$$

A plot of $\ln K_e$ against $1/T$ gives a straight line whose slope and intercept can be used to calculate the enthalpy and entropy respectively.

1.4 Adsorption Isotherms

Adsorption isotherms represent the amount of adsorbate adsorbed on the adsorbent's surface as a function of pressure (for gaseous fluids) at a constant temperature. For liquids, adsorption isotherms are represented as the amount of adsorbate as a function of its concentration. A number of isotherms exist, and are applied for many sorption processes. Below are some of the most common ones.

1.4.1 Langmuir Isotherm

First published in 1916 by Irving Langmuir[29], the Langmuir expression is one of the widely used isotherms for analyzing physical adsorptions. The semi-empirical isotherm, whose plot is shown in figure 1.2, is based on the following assumptions:

- A monolayer of adsorbate is formed homogeneously on the adsorbent surface.
- No interaction between the adsorbed molecules.
- Homogeneity of adsorption sites, and each site accommodates only one sorbate molecule.

The isotherm is mathematically expressed as:

$$Q = \frac{Q_{max} K_L c}{1 + K_L c} \tag{1.17}$$

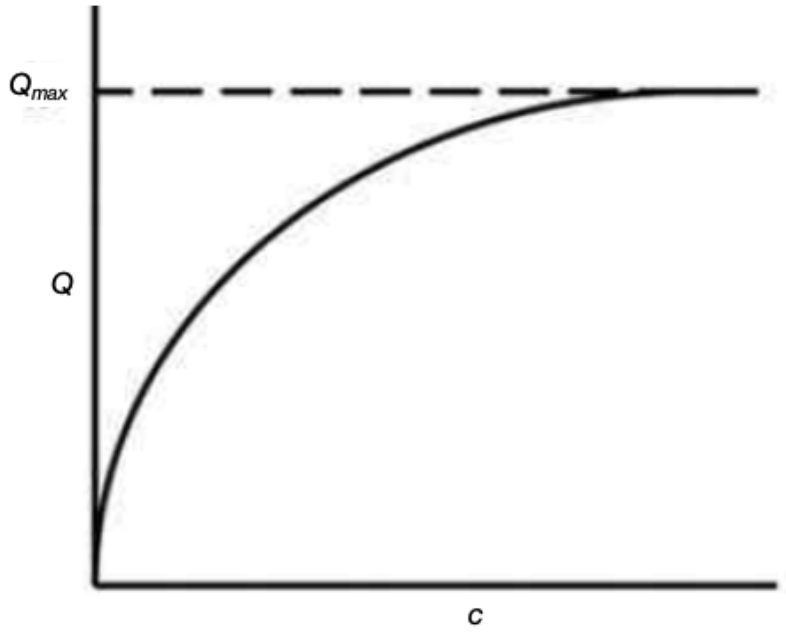

Figure 1.2: A plot of Langmuir Adsorption Isotherm

in which Q (mg/g) represents the mass of adsorbate adsorbed per unit mass of adsorbent, Q_{max} (mg/g) is the the maximum adsorption capacity (to form an adsorbate monolayer), c (mg/g) represents the equilibrium concentration of adsorbate in solution, and K_L (L/mg) is the Langmuir constant. In linear form, equation 1.17 is represented as

$$\frac{1}{Q} = \frac{1}{Q_{max}K_L}\frac{1}{c} + \frac{1}{Q_{max}} \tag{1.18}$$

whose plot of $1/Q$ against $1/c$ can be used to calculate values of Q_{max} and K_L from the intercept and slope respectively. A dimensionless constant, R_L shown in equation 1.19, known as the *separation factor*, specifies whether or not the adsorption method is favorable.[18] It is favorable for R_L values between 0 and 1, and unfavorable when R_L is greater than 1.

$$R_L = \frac{1}{1 + K_L c_o} \tag{1.19}$$

Here, c_o indicates the initial concentration.

1.4.2 Freundlich Isotherm

Empirically developed by Hebert Freundlich and Küster in 1909, the Freundlich adsorption isotherm is the oldest and arguably the most commonly used isotherm.[25] It is usually applicable for adsorption processes where the adsorbent exhibits non-uniform sites and energy distributions. Unlike Langmuir isotherm, the Freundlich isotherm is applicable for multi-layer adsorbate build-up on the adsorbent surface. Since the isotherm is capable of covering a wider range of concentration values than the Langmuir, it is usually sought in the analysis adsorption. It is mathematically represented as:

$$Q_e = K_f c^{1/n} \tag{1.20}$$

or linearly as:

$$\log Q_e = \log K_f + \frac{1}{n} \log c \tag{1.21}$$

where c represents the equilibrium concentration of adsorbate in solution, Q_e i.e., the mass of adsorbate adsorbed, and K_f is the adsorption capacity of adsorbent while n shows the adsorption intensity.

1.4.3 The Brunauer-Emmet-Teller(BET) Isotherm

The BET isotherm is based on the assumption that adsorption takes places at specific sites. It is favorable for multi-later sorbate build-up onto the adsorbent surface. For each layer, Langmuir isotherm is favorable. It is represented mathematically by the following equation:

$$Q = \frac{Q_{max} K_B c}{(c_s - c)[1 + (K_B - 1)(c/c_s)]} \tag{1.22}$$

where c_s (mg/L) is solubility limit (or saturation concentration) of solute, and K_B is a parameter related to the binding intensity of the layers.

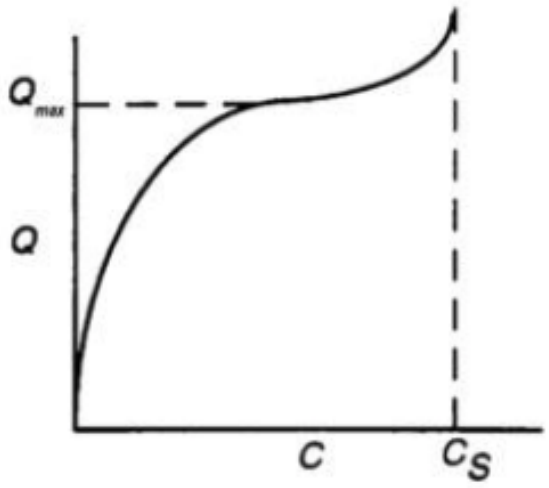

Figure 1.3: A plot of BET Adsorption Isotherm

1.4.4 Dubinin–Radushkevich (D-R) Isotherm

The D-R isotherm is applicable for heterogeneous surfaces of microporous adsorbents. It is a temperature dependent isotherm which "follows a pore-filling mechanism."[18] It follows a Gaussian-type distribution on heterogeneous surface, and is expressed mathematically as:

$$\ln Q_e = \ln Q_s - \beta\varepsilon^2 \tag{1.23}$$

in which β (mol^2/kJ^2) represents the Dubinin–Radushkevich isotherm constant, Q_s(mg/g) is theoretical isotherm saturation capacity, and ε is the equilibrium relation of adsorbate–adsorbent expressed as:

$$\varepsilon = RT \ln (1 + 1/c_s) \tag{1.24}$$

A plot of $\ln Q_e$ and ε^2 is a straight line whose slope and intercept can be used to calculate β and Q_s respectively.

Other isotherms that are usually sought for adsorption analyses include: Jovanovic adsorption isotherm, Hill adsorption isotherm, Elovich adsorption isotherm, Redlich–Peterson(R-P) adsorption isotherm etc.,

1.5 Literature Review

Different studies have been conducted and many models describing isothermal and non-isothermal adsorptions have been proposed. This chapter is aimed to introduce and analyze some of the existing non-isothermal adsorption models; and the succeeding chapter will give a thorough assessment of the work specific to MOFs. A general isothermal model and non-isothermal models are presented herein.

1.5.1 Isothermal Model

In many adsorption experiments, diffusivity determination from the traditional transient uptake curves is under the assumption that the process is isothermal. For a single spherical porous adsorbent particle exposed to a step change in sorbate concentration, it is generally assumed that heat transfer is very fast relative to the sorption rate; and temperature gradients within the particle, and to the surrounding ambient fluid are negligible,[19] thus heat transfer resistances can be neglected. In addition, if the fluid only contacts with the adsorbent particle at the surface ($r = r_0$), a constant intraparticle diffusivity, D_e, can be assumed[15]; and mass transport in the spherical particle can sufficiently be modeled using equations (1.25) and (1.26) below. Equation (1.25), which is Fick's second law, represents the rate of change of gas concentration at any given point within the particle volume.

$$\frac{\partial q}{\partial t} = D_e \left(\frac{\partial^2 q}{\partial r^2} + \frac{2}{r} \frac{\partial q}{\partial r} \right) \tag{1.25}$$

$q(r,t)$ quantifies the adsorbed gas concentration at radius r of the particle, and at time t. If the sorbate uptake is assumed to be negligible compared to the amount of sorbate introduced around the particle, then the sorbate concentration in the system remains fairly constant. Based on these assumptions, the following initial and

boundary conditions in equation (1.26)[19] hold.

$$q\,(r,0)\;=\;q_0'\;,\qquad\qquad q\,(r_0,t)\;=q_0\,,\qquad\qquad \left(\frac{\partial q}{\partial r}\right)_{r=0}\;=\;0 \tag{1.26}$$

It follows that the solution to equation (1.25), developed by Crank[4], is given by:

$$\frac{\overline{q}\;-\;q_0'}{q_0\;-\;q_0'}\;=\;\frac{\Delta M_t}{\Delta M_\infty}\;=\;1-\frac{6}{\pi^2}\sum_{n=1}^{\infty}\frac{1}{n^2}\,exp\left(\frac{-\pi^2 n^2 D_e\,t}{r_0^2}\right) \tag{1.27}$$

$\overline{q}$ in the uptake curve equation above defines the average adsorbed gas concentration[19] in the particle at a given time, expressed as:

$$\overline{q}(t)\;=\;\frac{3}{r_0^3}\int_0^{r_0} qr^2\,dr \tag{1.28}$$

However, assuming this isothermal behavior is only valid only for slow sorption rates.[19] Actually, not accounting for the heat generation during adsorption, like in equation (1.27), gives diffusivity values which are at variance with those obtained using methods like Nuclear Magnetic Resonance (NMR), a method recently applied to study diffusion and corresponding diffusivities. Recent studies have been aimed to provide an analysis of the thermal effects in adsorption measurements, and non-isothermal models have been presented.

1.5.2 Non-isothermal Models

Being an exothermic process, adsorption is usually characterized with large heat generations, especially in rapidly diffusing systems. The heat released causes a significant temperature increase within the particle, especially if it is not rapidly dissipated to the surrounding. This changes the kinetics of adsorption system, resulting into varying diffusivities of the same adsorbent material, which invalidates the isothermal assumption. These discrepancies have invoked a lot of research centered around non-isothermal adsorption to address the inconsistencies, and a number of mathematical models describing have resulted. Some of the resultant models presented below

also differ from each other significantly– each holds for different assumptions like: insignificant heat conduction in the particle (isothermal particle); infinite thermal conductivity of the adsorbent; among others.

(a) Lee and Ruthven (1979)

In this model, a single porous adsorbent particle is considered, for which only the intraparticle diffusion is assumed to be the dominant (and thus the rate-controlling) resistance to mass transport; and the equilibrium adsorbed phase concentration and diffusivity are assumed to be dependent on temperature.[20] The particle is considered to be isothermal since heat conduction in the particle is much faster than heat transfer at the surface.[12] Also, an infinite thermal conductivity is assumed so that temperature throughout the particle is fairly uniform. With these approximations, with a small differential step change in sorbate (fluid) concentration around the particle, equations (1.25), (1.28), (1.29), and (1.30) describe the mass and heat transfers, i.e.,

$$-\Delta H \frac{d\overline{q}}{dt} = c_s \frac{dT}{dt} + ha\,(T - T) \tag{1.29}$$

$$q\,(r,0) = 0\ , \qquad \frac{\partial q}{\partial r}(0,t) = 0 \tag{1.30}$$

in which ΔH is the heat of adsorption(negative), c_s is the heat capacity of the adsorbent, h is the overall heat transfer coefficient between the particle and the ambient gas, and a is the external surface area per unit volume.

The equilibrium relationship at the particle surface is assumed to be linear, and the equilibrium line is given by equation (1.31).[19]

$$\frac{q' - q'_0}{q_0 - q'_0} = 1 + \left(\frac{\partial q^*}{\partial T}\right)_P \left(\frac{T - T_0}{q_0 - q'_0}\right) \tag{1.31}$$

where the $(\partial q^*/\partial T)_P$ is the slope—taken to be constant over the step. The

uptake curve is given by the expression (1.32).[19]

$$\frac{\Delta M_t}{\Delta M_\infty} \;=\; 1 - \sum_{n=1}^{\infty} \frac{9\,[\,(p_n\,cot\;p_n - 1)/\,p_n^2\,]^2\;exp(-p_n^2\,D_e\;t/\,r_o^2)}{\frac{1}{\beta} + \frac{3}{2}\,[\,p_n\,cot\;p_n\,(p_n\,cot\;p_n - 1)/p_n^2\;\;+1]} \tag{1.32}$$

p_n in the equation is given by the roots of the equation:

$$3\beta\,(\,p_n\,cot\;p_n\;-\;1)\;\;=\;\;p_n^2\;-\;\alpha \tag{1.33}$$

in which

$$\beta\;\;=\;\;\frac{\Delta H}{c_s}\left(\frac{\partial q^*}{\partial T}\right)_P, \qquad\qquad \alpha\;\;=\;\;\frac{ha}{c_s}\frac{r_o^2}{D_e} \tag{1.34}$$

The corresponding temperature profile is given by:

$$\left(\frac{T - T_0}{q_0\;-\;q_0'}\right)\left(\frac{\partial q^*}{\partial T}\right)_P = \sum_{n=1}^{\infty} \frac{-3\,[\,(\,p_n\,cot\;p_n - 1)/\,p_n^2\,]\;exp(-p_n^2\,D_e\;t/\,r_o^2)}{\frac{1}{\beta} + \frac{3}{2}\,[\,p_n\,cot\;p_n\,(p_n\,cot\;p_n - 1)/p_n^2\;\;+1]} \tag{1.35}$$

When $\beta \to 0$ or $\alpha \to 0$, the roots of the equation (1.33) reduce to $p_n = n\pi$, and the non-isothermal uptake equation, (1.32), reduces to the isothermal expression in equation (1.27).[12]

(b) Sun and Muenier

In this model, a finite thermal conductivity is considered. However, it is differs from the above model in what the driving force of diffusion is considered to be. In Ruthven's model, diffusion follows the Fickian equation whereas in this model, gradient of chemical potential of the vapor phase (approximated to be an ideal gas) is the driving force. Additionally, in the previous Ruthven's model, only gas phase diffusion is considered while in this model, both vapor and adsorbed phase diffusion are considered. The model is based on the following conditions: intracrystalline diffusion is the dominant mass transfer resistance; mass diffusion in the pore volume occurs due to surface diffusion of adsorbed gas molecules as well as pore diffusion; adsorption rate is controlled by diffusion within the pore network, and not the surface adsorption kinetics.[23] The vapor

concentration, c, adsorbed concentration, q and temperature, T, are related by equation (1.36), in which $\mathrm{P}(q,T)$ is pressure of both phases, defined by Dubinin's equation presented in Meunier.[23]

$$c = \frac{\varepsilon - q/\rho_a}{RT}\, P(q,T) \tag{1.36}$$

After a few mathematical processes, the heat and mass transfers are expressed by the equations 2.13 – 2.18 below (all extracted from Meunier[23]):

$$\left[1 + \left(\frac{\partial c}{\partial q}\right)_T\right] \frac{\partial q}{\partial t} + \left(\frac{\partial c}{\partial T}\right)_q \frac{\partial T}{\partial t} = \frac{D}{r^2}\frac{\partial}{\partial r}\left[r^2\left(\frac{\partial q}{\partial r} + \delta\,\frac{\partial T}{\partial r}\right)\right] \tag{1.37}$$

$$\frac{\Delta H}{\rho_0 c_s}\left(\frac{\partial c}{\partial q}\right)_T \frac{\partial q}{\partial t} + \left[1 + \frac{\Delta H}{\rho_0 c_s}\left(\frac{\partial c}{\partial T}\right)_q\right] \frac{\partial T}{\partial t} = \frac{a_q + \delta D_V \Delta H/\rho_0 c_s}{r^2}\frac{\partial}{\partial r}\left(r^2\frac{\partial T}{\partial r}\right) + \frac{D_V \Delta H}{\rho_0 c_s}\frac{1}{r^2}\frac{\partial}{\partial r}\left(r^2\frac{\partial q}{\partial r}\right) \tag{1.38}$$

Initial conditions:

$$q = q_0\,, \qquad T = T_0\,, \qquad when \quad t = 0 \tag{1.39}$$

Boundary conditions:

$$\left(\frac{\partial q}{\partial r}\right)_{r=0} = 0\,, \qquad \left(\frac{\partial T}{\partial r}\right)_{r=0} = 0\,, \tag{1.40}$$

$$P_0 + \left(\frac{\partial P}{\partial q}\right)_T (q\,|_{r=r_0} - q_0) + \left(\frac{\partial P}{\partial T}\right)_q (T\,|_{r=r_0} - T_0) = P_1\,, \tag{1.41}$$

$$-\lambda\left(\frac{\partial T}{\partial r}\right)_{r=r_0} + h(\,T_1 - T\,|_{r=r_0}) = -\Delta H\, D_a\left[\left(\frac{\partial q}{\partial r}\right)_{r=r_0} + \delta\left(\frac{\partial T}{\partial r}\right)_{r=r_0}\right] \tag{1.42}$$

in which $a_q = \lambda\,/\rho_0 c_s$ defines the adsorbent's thermal diffusivity.

where the effective diffusion coefficients for the two phases, $D = D_a + D_V$, and

$$\delta = \frac{\left(\frac{\partial \mu}{\partial T}\right)_q}{\left(\frac{\partial \mu}{\partial q}\right)_T} \tag{1.43}$$

μ defines the chemical potential.

Upon change of variables, and performing Laplace transforms, the corresponding average sorbate concentration and temperature profile (respectively) in the particle are given by equations (1.44) and (1.45)[23]:

$$\overline{\omega} = 1 + \sum_{n=1}^{\infty} \frac{6Su\ exp(-p_n^2\tau)}{p_n\, Q(p_n)} \left[A_1 P_2(p_n) \left(-\frac{cos(b_1 p_n)}{b_1 p_n} + \frac{sin(b_1 p_n)}{(b_1 p_n)^2} \right) - A_2 P_1(p_n) \left(-\frac{cos(b_2 p_n)}{b_2 p_n} + \frac{sin(b_2 p_n)}{(b_2 p_n)^2} \right) \right] \tag{1.44}$$

$$\overline{\theta} = 1 + \sum_{n=1}^{\infty} \frac{2Su\ exp(-p_n^2\tau)}{\eta\, p_n\, Q(p_n)} \left[P_2(p_n) sin(b_1\, \eta\, p_n) - P_1(p_n) sin(b_2\, \eta\, p_n) \right] \tag{1.45}$$

Details regarding the simple derivations of these concentration and temperature profiles, along with the included reduced variables and dimensionless parameters are presented in Meunier.[23] The *Appendix* of referenced work presents the solutions of the above linear differential system using Laplace transforms.

This model would be sufficient for the non-isothermal adsorption analysis of CO_2 in a MOF particle, however, the available information on some parameters is insufficient for adsorbent to allow for a thorough study.

For this model, the isothermal case is justified when the the Lewis number, *Le*, is greater than 10, in which case heat conduction in the particle is rapid enough to assume uniform temperature profile. A more straightforward and clearer model which gives fairly uniform results, was used in the analysis.

(c) Haul and Stremming's Model

The model is based on the following assumptions quoted from Haul[7]:

- Both vapor and adsorbed phase diffusion occur—within the pore volume and at the pore surface. They are defined and related by the following equations:

$$\left(\frac{\partial q}{\partial c}\right)_T = \beta = \frac{1-\epsilon}{\epsilon}\rho_0 RT \left(\frac{\partial n}{\partial p}\right)_T \tag{1.46}$$

$$\left(\frac{\partial q}{\partial T}\right)_c = -\alpha \tag{1.47}$$

$$\frac{\partial q}{\partial t} = \beta\frac{\partial c}{\partial t} - \alpha\frac{\partial T}{\partial t} \tag{1.48}$$

  in which β and α respectively define the slopes of the adsorption isotherm and isobar, and ϵ represents the adsorbent's porosity.

- The total coefficient of diffusion is independent of temperature and concentration over over a sorption step

- Constant effective thermal conductivity, heat of adsorption, specific heat capacity of the adsorbent with adsorbate, density, and heat transfer coefficient over the adsorption step.

Based on these assumptions, the following differential equations (quoted from Haul[7] describe mass and heat transfers for the adsorption process.

$$\frac{\partial c}{\partial t} + \frac{\partial q}{\partial t} = D_e\left(\frac{\partial^2(c+q)}{\partial r^2} + \frac{2}{r}\frac{\partial\,(c+q)}{\partial r}\right) \tag{1.49}$$

$$\rho_0 c_s\frac{\partial T}{\partial t} = \Delta H\frac{\partial q}{\partial t} + \lambda\left(\frac{\partial^2 T}{\partial r^2} + \frac{2}{r}\frac{\partial\,T}{\partial r}\right) - \frac{3h}{r_0}(T - T_0) \tag{1.50}$$

It is apparent from equations (1.49) and (1.50) that q, c, and T are functions of r and t.

The following initial and boundary conditions can sufficiently be applied to solve

the system of differential equations.

$$q = q_\infty\ , \qquad c = c_\infty\ ; \qquad\qquad r = r_0,\ t > 0$$

$$q = q_0'\ , \qquad c = c_0'\ ; \qquad 0 \le r \le r_0,\ t = 0$$

$$q = q_\infty\ , \qquad c = c_\infty\ ; \qquad 0 \le r \le r_0,\ t \to \infty$$

$$\Delta T\ = T - T_0 = 0; \qquad 0 \le r \le r_0,\ t = 0\,,\, t \to \infty$$

$$\Delta T\ = T - T_0 = 0; \qquad r = r_0,\ t \ge 0$$

After a few easy integration steps, the resultant mean adsorbate concentration and average temperature difference profiles at a given time in the particle are given by the equations:

$$\frac{M_t\ -\ M_0}{M_\infty -\ M_0} = \frac{\Delta M_t}{\Delta M_\infty}\ =\ 1 - \frac{6}{\pi^2}\sum_{n=1}^{\infty}\frac{1}{n^2}\left[1 + t\left(p_n\ - \frac{\pi^2 n^2 D_e\, F}{r_0^2\,(F + \alpha - \beta E)}\right)\right] exp(-p_n t) \tag{1.51}$$

$$\overline{\Delta T}(t) = \frac{6}{r_0^2}\,(M_\infty -\ M_0)\sum_{n=1}^{\infty}\frac{\rho_0 t D_e}{(F + \alpha - \beta E)}\,exp(-p_n t) \tag{1.52}$$

with

$$p_n = \frac{\pi n}{r_0}\sqrt{\frac{D_e}{(F + \alpha - \beta E)}\left(\frac{\pi^2 n^2 H}{r_0^2 +} + G\right)} \tag{1.53}$$

$$E = \frac{\alpha}{1+\beta}\ , \qquad F = \frac{\rho_0 c_s}{\Delta H}\,, \qquad G = \frac{3h}{r_0 \Delta H}\,, \qquad H = \frac{\lambda}{\Delta H}\,, \qquad \overline{\Delta T} = \overline{T} - T_0$$

where T_0 represents the initial particle temperature, while $\overline{T}$ the average particle temperature at any given time during the process, M_0 defines the amount adsorbed at *t=0*, M_t is the amount adsorbed at a given time, and M_∞ is the amount of sorbate at equilibrium. Both the average sorbate concentration and mean temperature difference expressions are functions of *t*.

1.6 Objective of the Analysis

Over and above, in a bid to address the increasing levels of CO_2 in the atmosphere, adsorption is being sought to accomplish both pre- and post- combustion CO_2 capture processes, which are key stages of the carbon capture and storage (CCS) technology in refineries, power plants and other industries. Consequently, a lot of research is being carried out to discover efficient and effective adsorption methods to cope with the growing demand to reduce CO_2 concentrations in our atmosphere.

Many of these studies are aimed at investigating adsorption parameters like adsorbent density, pore diameters, adsorbate uptakes, adsorption isotherms, diffusivity; and enthalpy of adsorption —a key indicator of the feasibility and extent of adsorption. Being a thermodynamically exothermic process, adsorption releases heat to the surrounding. Therefore, it is paramount to have a clear and thorough understanding of such properties for CO_2 adsorption on MOF-5 using an appropriate model. Unfortunately, some properties are overlooked in many studies. In Muenier's work, an infinite effective thermal conductivity is assumed, which makes temperature in the particle uniform; yet CO_2 / MOF-5(Molybdenum pentafluoride) system has a finite value of thermal conductivity. While Stremming non-isothermal model considers a finite thermal conductivity, it is limited by its suitability for mesoporous adsorbents, and by the assumption that diffusivity is constant during the process.

The objective of this paper is to introduce a new model suitable for the analysis of the non-isothermal CO_2 adsorption on the microporous MOF-5 particle, with the assumption of finite effective thermal conductivity as well as varying diffusivity.

Chapter 2

ANALYSIS OF ADSORPTION USING EXISTING MODELS

In the study of diffusion and adsorption of CO_2 on MOF particles presented in Zhao [31], just like in other studies, the non-isothermal nature of adsorption on the porous adsorbent is not accounted for, let alone the resulting temperature changes that actually take place during the process. In addition, for the isothermal case reported by Zhao, the analysis is carried out using Crank's equation for short sorption times, which is ideal for use only for isothermal processes.

The purpose of this chapter is to present different analyses of adsorption in porous adsorbent particles for both isothermal and non-isothermal cases. Haul and Stremming's model[7] in equations (1.51)—(1.53) is deployed for the analysis of the non-isothermal case, while for the isothermal part, the derived equation (2.6) , in lieu of Crank's equation (1.27)[4], is used to accomplish the analysis. The differences between Crank's and the derived isothermal models are showed in *Chapter 4*. The models' key parameters and their effects on the respective adsorption uptakes and average temperature differences are studied. The models are employed to study the adsorption of CO_2 on MOF-5, in Zhao's [31] experiment; considering both isothermal and nonisothermal cases.

2.1 Analysis Models

In this section, the isothermal model equations previously alluded to, as well as the non-isothermal model are presented. These models are used to accomplish the analyses of adsorption processes.

2.1.1 Haul and Stremming Non-isothermal Model

In this analysis, Haul and Stremming[7] presented an experiment for the adsorption of benzene into a mesopore porous silica gel particle as a test system. The parameters used in the calculations are defined and given in Table C.1.

The specific heat capacity, c_s, is calculated from (2.1):

$$c_s = \frac{m_1 c_{s1} + m_2 c_{s2}}{m_1 + m_2} \qquad (i)$$

$$(m_1 + m_2)\, c_s = m_1 c_{s1} + m_2 c_{s2}$$

$$m_1 c_{s1} = m_2 c_{s2} \qquad (ii)$$

$$(m_1 + m_2)\, c_s = 2\, m_1 c_{s1}$$

$$c_s = \frac{2\, c_{s1}}{1 + m_2/m_1} \qquad (iii)$$

From (ii), equation (iii) becomes:

$$c_s = \frac{2\, c_{s1} c_{s2}}{c_{s1} + c_{s2}}$$

Thus, the specific heat of the system is:

$$c_s = \frac{2\, c_s(SiO_2)\ c_s(C_6H_6)}{c_s(SiO_2) + c_s(C_6H_6)} \qquad (2.1)$$

The conduction heat transfer coefficient, h(cond), is calculated using

$$h(cond) = \frac{Nu\lambda_g}{2r_0} \qquad (2.2)$$

while the radiation heat transfer coefficient, h(rad), is got from:

$$h(rad) = \frac{4\sigma\, {T_0}^3}{1/e_1 + 1/e_2 - 1} \qquad (2.3)$$

The corresponding isothermal and non-isothermal uptake profiles are shown

using the now already familiar equations (1.27)[for long times] and (1.51) respectively, while the average particle temperature changes associated with the non-isothermal case can be determined using equation (1.52). The respective plots of these equations are shown in Figure 2.1.

2.1.2 Isothermal Model from Stremming's Uptake Equation

For comparison with the non-isothermal uptake curve in equation (1.51), a different isothermal uptake curve is derived and used instead of Crank's equation. This is centrally because Crank's (1.27) and Stremming nonisothermal equation (1.51) are derived using different methods. Moreover, obtaining Crank's isothermal curve from Stremming non-isothermal equation is not possible. An isothermal equation, therefore, is derived from Stremming non-isothermal equation (as shown below) to accomplish the comparison.

From equations (1.51) and (1.53), after substitution, the Stremming's equation can be written as:

$$\frac{\Delta M_t}{\Delta M_\infty} = 1 - \frac{6}{\pi^2}\sum_{n=1}^{\infty}\frac{1}{n^2}\left[1 + t\left(\frac{\pi n\, A}{r_0} - \frac{\pi^2 n^2 D_e c_s \rho_e}{\Delta H r_0^2\left(\alpha - \frac{\alpha\beta}{\beta+1} + \frac{c_s\,\rho_e}{\Delta H}\right)}\right)\right] exp\left(-\frac{\pi n t\, A}{r_0}\right) \tag{2.4}$$

where

$$A = \sqrt{\frac{D_e\left(\frac{3h}{\Delta H r_0} + \frac{\lambda_e \pi^2 n^2}{\Delta H r_0^2}\right)}{\alpha - \frac{\alpha\beta}{\beta+1} + \frac{c_s\,\rho_e}{\Delta H}}}$$

Consider a scenario where n = 1. Since the temperature is constant i.e., $\Delta T = 0$ for an isothermal process, the change in heat of adsorption is zero, and the limit as $\Delta H \to 0$ can be taken for equation (2.4), which becomes:

$$\frac{\Delta M_t}{\Delta M_\infty} = \lim_{\Delta H \to 0} \left[1 - \frac{6}{\pi^2} \left(1 + t \left(\frac{\pi\, A'}{r_0} - \frac{\pi^2 D_e c_s \rho_e}{\Delta H r_0^2 \left(\alpha - \frac{\alpha\beta}{\beta+1} + \frac{c_s\, \rho_e}{\Delta H} \right)} \right) \right) exp \left(-\frac{\pi t\, A'}{r_0} \right) \right] \tag{2.5}$$

where

$$A' = \sqrt{\frac{D_e \left(\frac{3h}{\Delta H r_0} + \frac{\lambda_e \pi^2}{\Delta H r_0^2} \right)}{\alpha - \frac{\alpha\beta}{\beta+1} + \frac{c_s\, \rho_e}{\Delta H}}}$$

For n = ∞, equation (2.5) becomes:

$$\frac{\Delta M_t}{\Delta M_\infty} = 1 - \frac{6}{\pi^2} \sum_{n=1}^{\infty} \frac{1}{n^2} \left[1 - \frac{D_e \pi^2 n^2 t + \pi\, n\, t\, r_0\, B}{r_0^2} \right] exp \left(-\frac{\pi n t\, B}{r_0} \right) \tag{2.6}$$

which is the isothermal curve, with

$$B = \sqrt{\frac{D_e \left(\lambda_e \pi^2 n^2 + 3 h r_0 \right)}{c_s \rho_e r_0^2}}$$

Similarly, taking the limit of equation (1.52) as $\Delta H \to 0$ clearly yields $\overline{\Delta T} = 0$, a confirmation for isothermal adsorption i.e.,

$$\overline{\Delta T}(t) = \lim_{\Delta H \to 0} \left[\frac{6}{r_0^2} \left(M_\infty - M_0 \right) \sum_{n=1}^{\infty} \frac{\rho_0 t D_e}{\left(\alpha - \frac{\alpha\beta}{\beta+1} + \frac{c_s\, \rho_e}{\Delta H} \right)} exp \left(-\frac{\pi n t\, A}{r_0} \right) \right] = 0 \tag{2.7}$$

The two isothermal equations (Crank's (1.27) and the Stremming derived isothermal (2.6)) give different uptake curves and $\Delta M_t / \Delta M_\infty$ values, as shown in figure 2.2 and table D.1, for the sorption of benzene into a silica gel particle experiment as a test example. Equation (2.6) instead of Crank's equation (1.27) is employed for isothermal analysis.

2.2 Parametric Analysis of the Models

From the model, the key parameters for both isothermal and non-isothermal cases, and their nominal values are r_0, ΔH, and D_e. The parametric study carried out is centered around these parameters. The parametric results which result into insignificant average temperature changes are reported.

(a) Effect of Heat of Adsorption, ΔH, on Uptake and $\overline{\Delta T}$

The models are used to study the effect of heat of adsorption, ΔH, on the uptakes for both isothermal and non-isothermal cases, as well as on the average temperature changes in the particle. ΔH values 4.19x10^4, 4.19x10^5, 83.8x10^5 and 167.6x10^5 J/mol are tested. The resulting uptakes and $\overline{\Delta T}$ are presented in the subsequent chapter.

(b) Effect of Particle Radius, r_0, on Uptake and $\overline{\Delta T}$

The size of the adsorbent particle affects both uptake values and the average temperature changes in the particle. Particles sizes 2.5 x 10^{-2}, 2.5 x 10^{-3}, and 2.5 x 10^{-4} m are studied at constant ΔH and De(non-isothermal) is 2.9 x 10^{-9} m^2/s. The results are shown in section 4.0.3.

(c) Effect of Diffusivity, D_e, on Uptake and $\overline{\Delta T}$

There is a positive impact of diffusivity on uptakes and the resultant particle temperature differences. The effect is studied by analyzing the model responses for increasing diffusivities, i.e, 2.3 x 10^{-9} (nominal value), 2.3 x 10^{-8}, and 2.3 x 10^{-7} m^2/s, at constant ΔH and r_0.

2.3 Results for Analysis for Benzene- Silica Gel Adsorption

From equation (2.1), the specific heat of silica gel-benzene system, c_s, is 1.0482 x 10^3 $Jkg^{-1}K^{-1}$. Using equations (2.2) and (2.3), h(cond) and h(rad) are 3.4 and 4.0789 $Wm^{-2}K^{-1}$ respectively, making the effective heat transfer coefficient, h = 7.4789 $Wm^{-2}K^{-1}$. The resulting uptake and temperature curves generated for the adsorption of benzene on a silica gel particle are shown in the figure below. From the uptake curves, the maximum average concentration of benzene in the

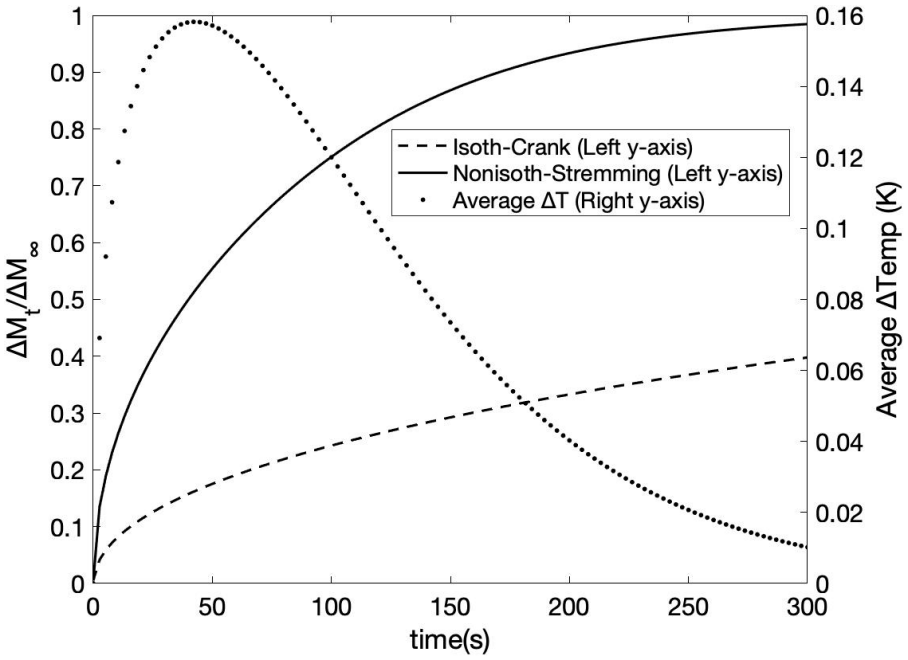

Figure 2.1: Uptakes & $\overline{\Delta T}$ for Adsorption of Benzene on Silica gel: r_o 2.5 x 10^{-3}m

silica gel particle, $\Delta M_t/\Delta M_\infty$ = 0.3978 and 0.9846 for isothermal and non-isothermal cases respectively, while the maximum mean temperature change in the particle, $\overline{\Delta T}$ = 0.1582 K. From the plot, the non-isothermal curve is faster than the isothermal uptake, an indication that the diffusivity used for isothermal case is lower than the actual value.

2.3.1 *Differences Between Non-isothermal and Isothermal Models*

As shown in the figure below, plots for Crank uptake curve and *Haul & Stremming* derived isothermal equation are different for the same diffusivity, D_e(iso) = 3.7 x 10^{-10} m^2/s for t = 300 seconds. Crank's uptake curve is slower, and takes longer to reach equilibrium than *Haul & Stremming* derived isothermal equation.

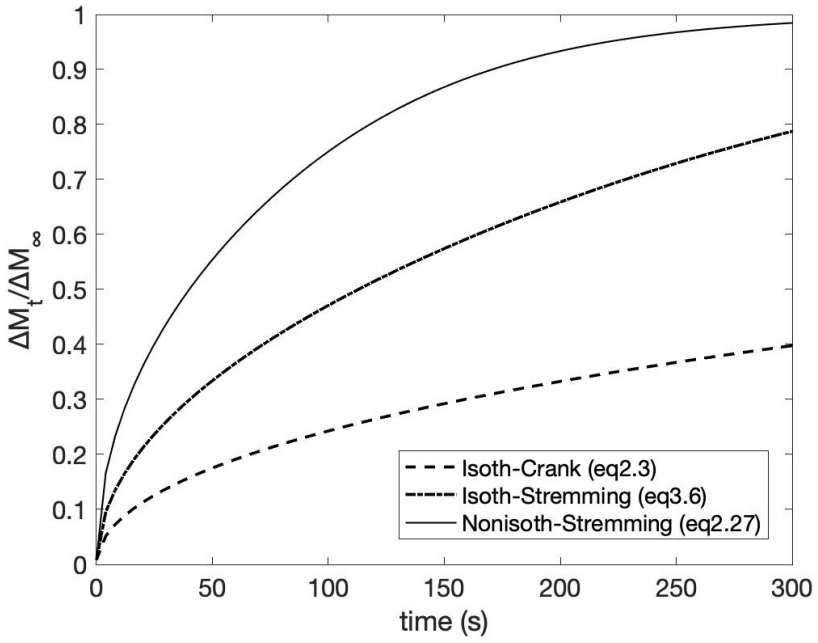

Figure 2.2: Isothermal & Non-isothermal Uptakes:D_e(iso)=3.7x10^{-10}, D_e(non): 2.3 x 10^{-9} m^2/s, r_o 2.5 x 10^{-3} m

However, the non-isothermal curve, plotted for D_e(non) = 2.3 x 10^{-9} m^2/s, is much faster than the two isothermal curves because it is plotted for a larger more actual diffusivity.

For the larger diffusivity, both *Haul & Stremming* isothermal and non-isothermal curves are similar as seen below:

The Stremming derived equation (2.6), thus, is the isothermal uptake curve

Table 2.1: Maximum Uptakes for D_e(iso): 3.7 x 10^{-10}, D_e(non), r_o 2.5 x 10^{-3} m

Uptake Curve	Max. Uptake Value ($\Delta M_t/\Delta M_\infty$)
Isothermal–Crank	0.3978
Isothermal–Stremming	0.7876
Non-isothermal–Stremming	0.9846

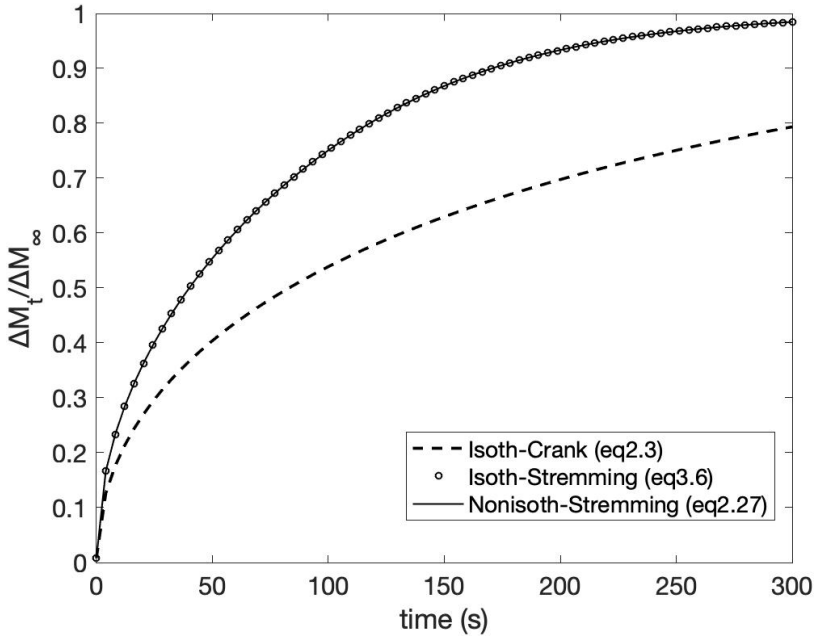

Figure 2.3: Isothermal and Non-isothermal Uptakes: D_e(non): 2.3 x 10^{-9} m^2/s, r_o 2.5 x 10^{-3} m

used for comparison with the Stremming non-isothermal curve in the subsequent analyses.

Table 2.2: Maximum Uptakes for D_e(non): 2.3 x 10^{-9} m^2/s, r_o 2.5 x 10^{-3} m

Uptake Curve	Max. Uptake Value ($\Delta M_t/\Delta M_\infty$)
Isothermal–Crank	0.7936
Isothermal–Stremming	0.9846
Non-isothermal–Stremming	0.9846

2.3.2 Effect of ΔH on Uptakes and $\overline{\Delta T}$

For diffusivity, D_e = 2.9 x 10^{-9} m^2/s, there's a significant impact of ΔH on both the benzene uptake and average particle temperature changes for non-isothermal case. As ΔH increases, the uptake curves become slower as shown in the plots below. The differences between the uptake curves are not much because, in the derivation of the Stremming uptake curve, it was assumed that D_e is independent of temperature, i.e., the increasing ΔH and thus increased $\overline{\Delta T}$ barely affect the uptake curves. In principle, D_e is dependent on temperature;

Table 2.3: Effect of ΔH on Uptake and $\overline{\Delta T}$:D_e(non)=2.3x$10^{-9}$$m^2/s$, r_o=2.5x10^{-3}m

ΔH (J/mol)	Max. $\Delta M_t/\Delta M_\infty$	Max. $\overline{\Delta T}$ (K)
41.9 x 10^4	0.9843	0.5750
41.9 x 10^5	0.9814	15.1827
83.8 x 10^5	0.9780	29.2184
167.6 x 10^5	0.9707	54.5651

and this is the frontier of this work in the subsequent chapters.

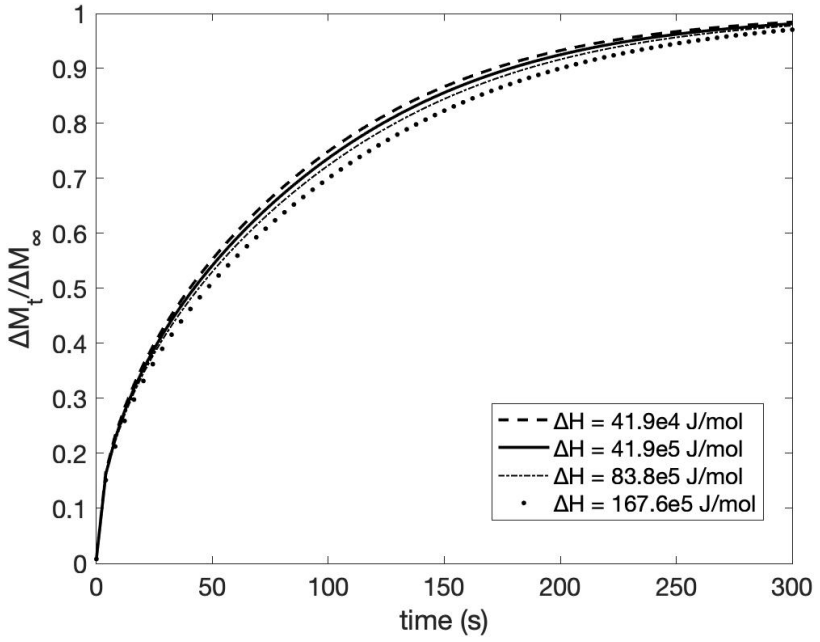

Figure 2.4: Effect of ΔH on Uptakes: D_e(non): 2.3 x 10^{-9} m^2/s, r_o 2.5 x 10^{-3} m

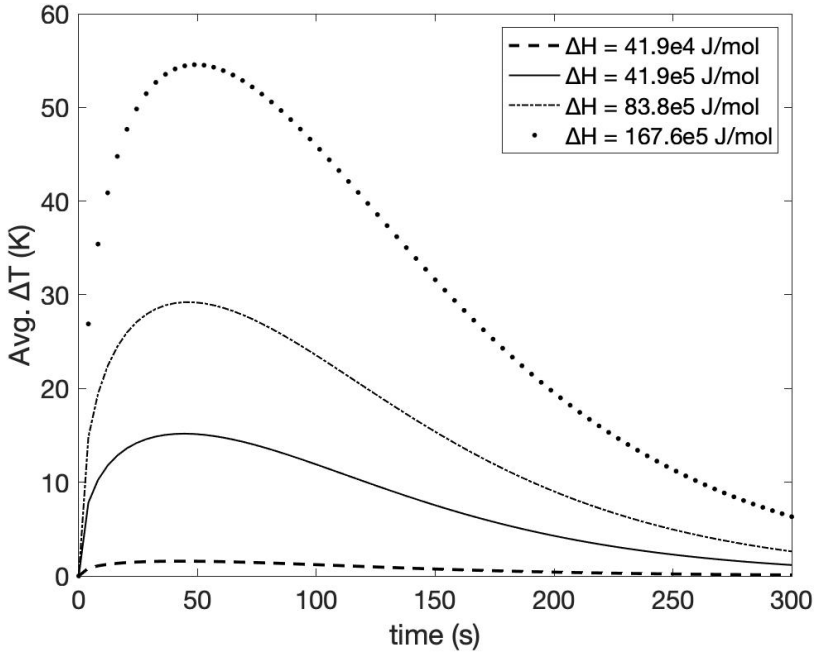

Figure 2.5: Effect of ΔH on $\overline{\Delta T}$: D_e(non): 2.3 x 10^{-9} m^2/s, r_o 2.5 x 10^{-3} m

Nevertheless, the maximum $\overline{\Delta T}$ increases with increasing ΔH. For small ΔH values, the resulting $\overline{\Delta T}$ values are so small that they can be regarded insignificant, and isothermal case can be assumed.The non-isothermal model becomes relevant for larger ΔH values (i.e, order of $10^{>=3}$) as shown in table 2.3 above.

2.3.3 Effect of Particle Radius, r_0, on Uptake and $\overline{\Delta T}$

The maximum benzene uptake increases with reducing particle radius at t = 10s, for D_e(non) is 2.9 x 10^{-9} m^2/s and ΔH = 41.9 kJ/mol. This trend can be attributed to the fact that for smaller particles, the diffusing adsorbent molecules are transported through the entire particle very fast, increasing the average sorbate concentration.

The average temperature difference in the particle, in the same manner, increases with decreasing particle size.

Table 2.4: Effect of r_0 on Uptake&$\overline{\Delta T}$:D_e=2.3x$10^{-9}$$m^2$/s,$\Delta H$=34.1x$10^4$J/mol,t=10s

r_0 (m)	Max. $\Delta M_t/\Delta M_\infty$	Max. $\overline{\Delta T}$ (K)
2.5 x 10^{-2}	0.0266	0.1482
2.5 x 10^{-3}(Nominal)	0.2576	1.1604
2.5 x 10^{-4}	1.000	1.6109

In the larger particle, the generated heat of adsorption is conducted over a wider distance to the particle surface, making the temperature profile slower.

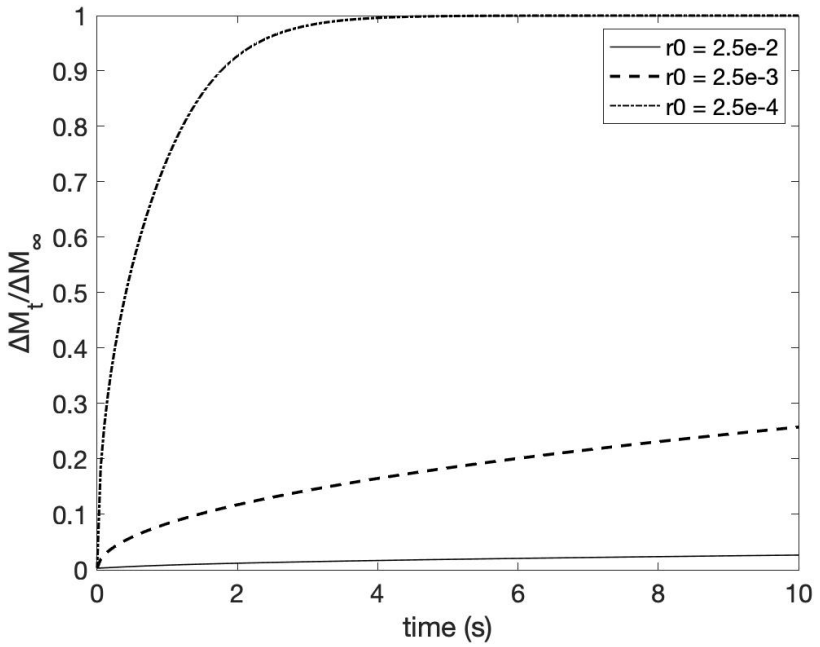

Figure 2.6: Effect of r_0 on Uptake:D_e(non):2.3x10^{-9} m^2/s, ΔH=34.1x10^{4}J/mol, t=10s

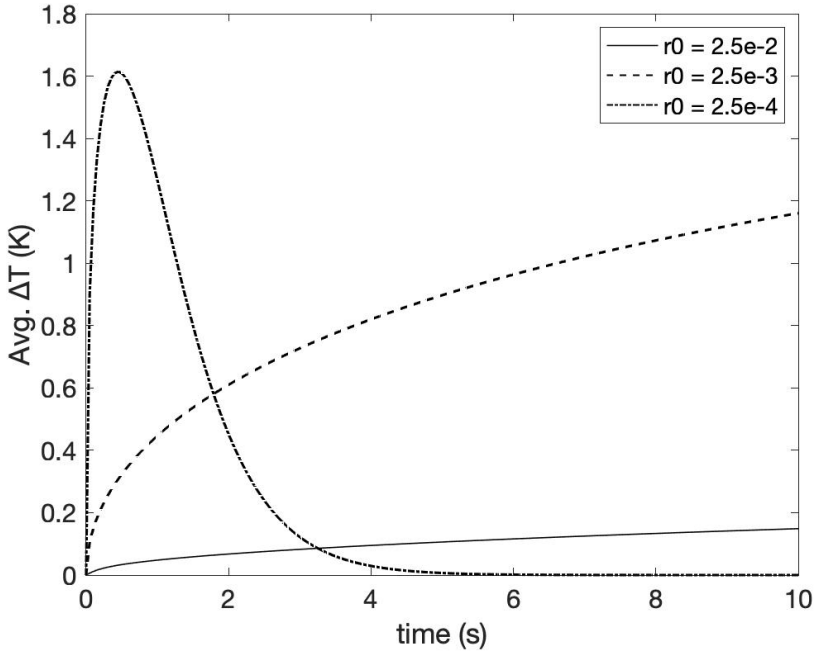

Figure 2.7: Effect of r_0 on $\overline{\Delta T}$:D_e(non):2.3x10^{-9}m^2/s,ΔH=41.9x10^{4}J/mol,t=10s

For a smaller particle, of radius 2.5 x 10^{-4} m for example, the the change in temperature in much larger and more rapid than that of radius 2.5 x 10^{-2} m. This is because in the smaller particle, diffusion throughout the particle is faster. The more the diffusion of the sorbate molecules, the higher the particle temperature. The temperature profile in the smaller particle (r_0 = 2.5 x 10^{-4} m) is also rapid, because the generated heat of adsorption is readily conducted to the surrounding, thus reducing the average particle temperature to about 0 K at t = 5 seconds.

Over a very long time, the slower curves for both uptake and $\overline{\Delta T}$ shoot up and their maximum values increase, at which time the curves for the smaller particle long reached equilibrium i.e., 1 for uptake curve and 0 K for temperature profile as seen in the table and plots below.

Table 2.5: Effect of r_0 on Uptake & $\overline{\Delta T}$:D_e=2.3x10^{-9}m^2/s,ΔH=34.1x10^4J/mol,t=100s

r_0 (m)	Max. $\Delta M_t/\Delta M_\infty$	Max. $\overline{\Delta T}$ (K)
2.5 x 10^{-2}	0.0837	0.4439
2.5 x 10^{-3}(Nominal)	0.7495	1.5758
2.5 x 10^{-4}	1.000	1.6089

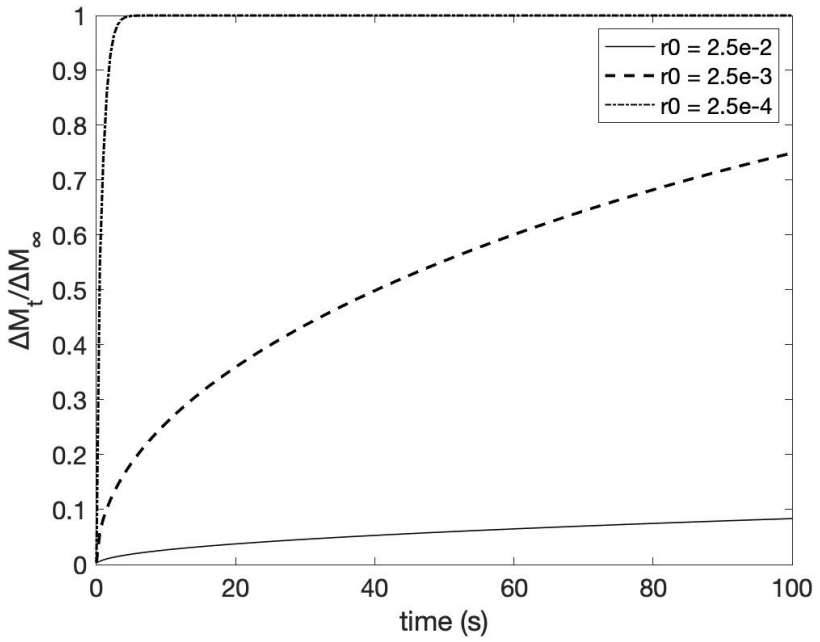

Figure 2.8: Effect of r_0 on Uptake: D_e(non): 2.3 x 10^{-9} m^2/s, ΔH = 41.9 x 10^4 J/mol, t = 100s

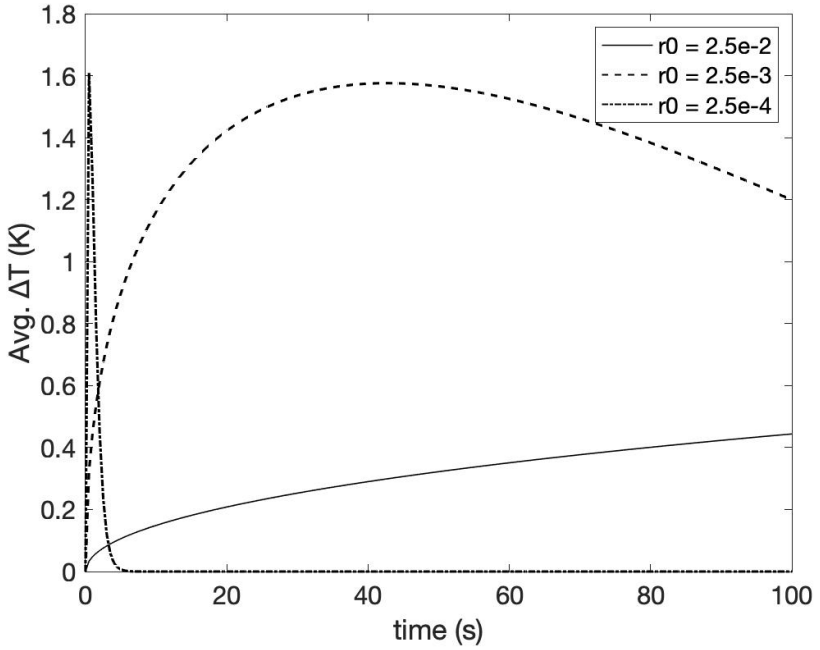

Figure 2.9: Effect of r_0 on $\overline{\Delta T}$: D_e(non): 2.3 x 10^{-9} m^2/s, ΔH = 41.9 x 10^4 J/mol, t = 100s

2.3.4 *Effect of Diffusivity, D_e, on Uptake and $\overline{\Delta T}$*

At the nominal value of r_0 and $\Delta H = 41.9 \times 10^4$ J/mol, the maximum uptake of benzene on silica gel at t = 300s increases with increasing diffusivity, D_e, and so does the average temperature difference. The higher the diffusivity, the faster the diffusion of benzene, and the faster the uptake. Ultimately, the average silica gel particle temperature increases due to increasing kinetic energy as a result of rapid movement of benzene molecules. As diffusivities reduce, $\overline{\Delta T}$ increasingly reduce; likely due to the reduced mobility of the benzene molecules through the porous network of silica gel particle, which reduces diffusion, and thus low kinetic energy of sorbate.

Table 2.6: Effect of D_e on Uptake & $\overline{\Delta T}$: ΔH=41.9x10^{4}J/mol,r_0=2.5x10^{-3}m,t=300s

D_e (m^2/s)	Max. $\Delta M_t/\Delta M_\infty$	Max. $\overline{\Delta T}$
2.3 x 10^{-9} (Nominal)	0.9843	1.5757
2.3 x 10^{-8}	1.000	4.9829
2.3 x 10^{-7}	1.000	15.7446

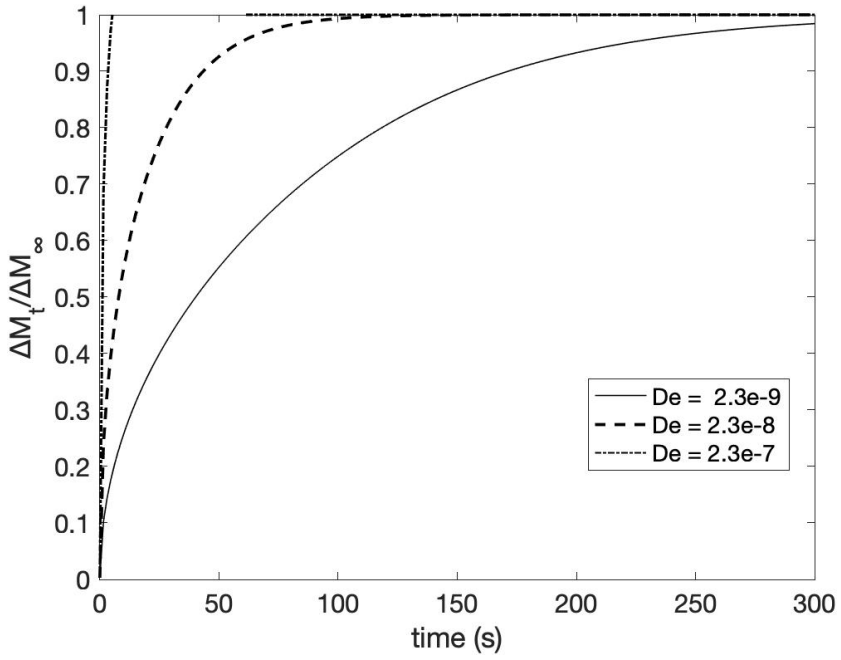

Figure 2.10: Effect of D_e on Uptake:ΔH=41.9x10^4 J/mol, r_0 = 2.5x10^{-3}m, t=300s

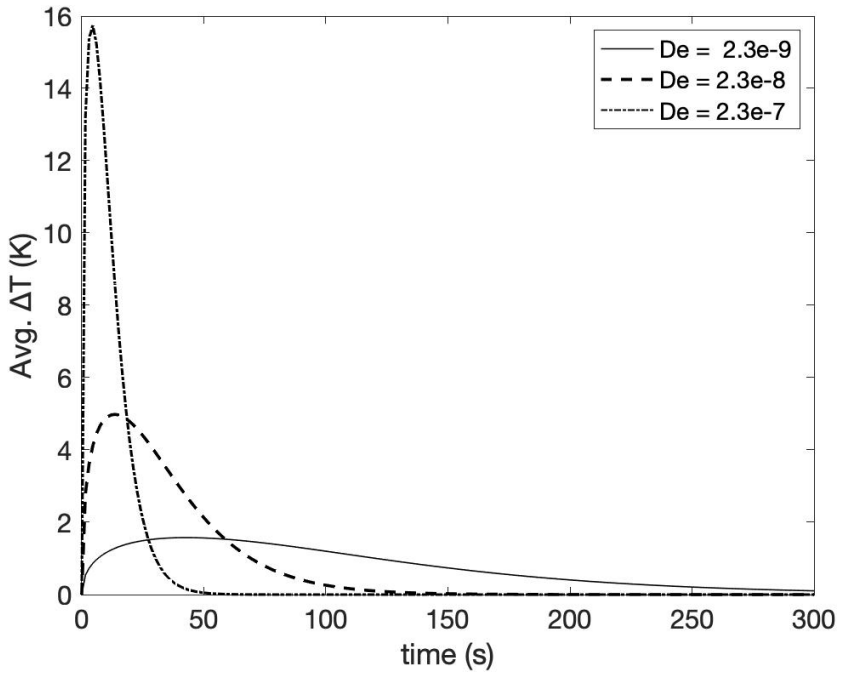

Figure 2.11: Effect of D_e on $\overline{\Delta T}$:ΔH = 41.9x10^4 J/mol, r_0 = 2.5x10^{-3} m,t = 300s

2.4 Results for CO_2 - MOF-5 Adsorption Using Existing Models

A similar analysis was carried for the adsorption of CO_2 gas on MOF-5. The parameters used are defined in the Appendix. Using equation (2.1), the specific heat of CO_2 -MOF-5 particle, c_s, is 814.90 $Jkg^{-1}K^{-1}$; and from equations (2.2) and (2.3), h(cond) and h(rad) are 646.8 and 2.8350 $Wm^{-2}K^{-1}$ respectively, making the effective heat transfer coefficient, h = 649.6350 $Wm^{-2}K^{-1}$. This value is quite to high, but it stems from the micro radius of the MOF particle under investigation. The resulting uptake curves and average temperature profiles generated are shown in the figure below. It should be noted that for this adsorption, because it is extremely fast at the given nominal values (shown in the Appendix), the curves are usefully visible for small time, t = 0.01s.

2.4.1 Uptake Curves — CO_2 Adsorption on MOF-5

From the table and graphs below, the Crank's uptake curve is way slower than the Stremming isothermal uptake curve, majorly because the diffusivity, D_e(iso) = 8.17 x 10^{-13} m^2/s is much smaller than what it should be; i.e., the one used for non-isothermal case, D_e(non) = 5.58 x 10^{-9} m^2/s, which leads to a faster uptake curve as shown in the plots below. The corresponding $\overline{\Delta T}$ that is achieved for non-isothermal case is 0.7278 K. This is indeed significant especially considering bed adsorption of MOF-5.

Table 2.7: Maximum Uptakes for Different Uptake Curves at t = 0.01s

Uptake Curve	Max. Uptake Value ($\Delta M_t/\Delta M_\infty$)
Isothermal–Crank	0.0158
Isothermal–Stremming	0.1936
Non-isothermal–Stremming	0.9999

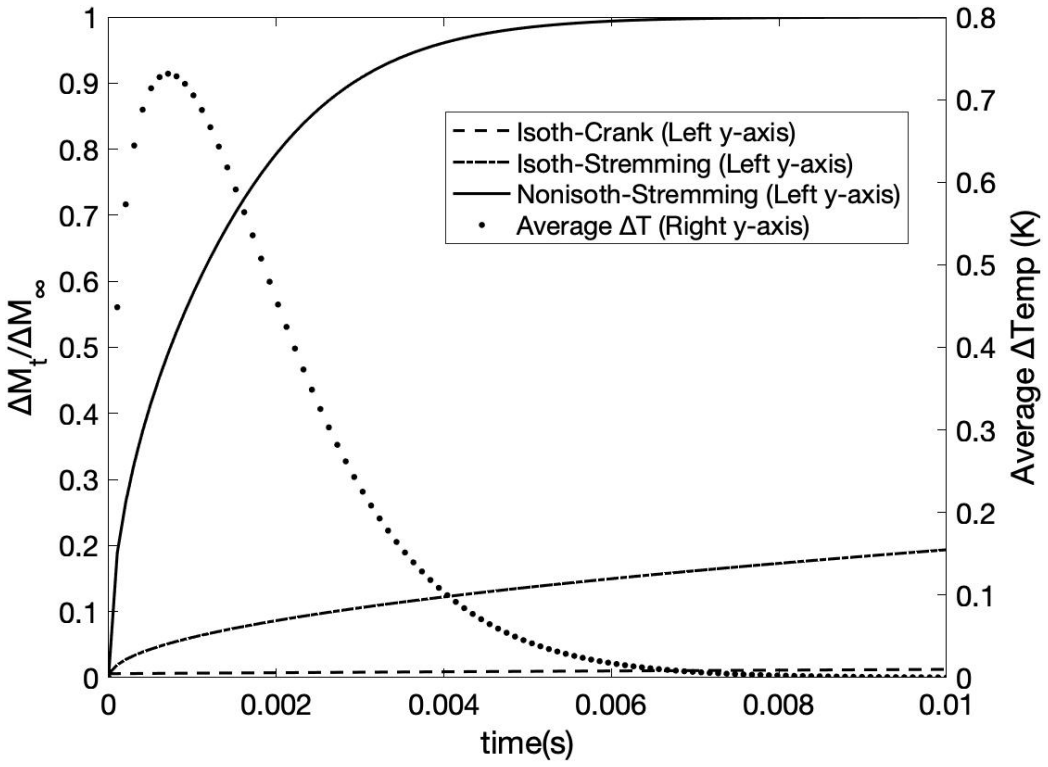

Figure 2.12: Isothermal and Non-isothermal Uptakes: D_e(iso): 8.17 x 10^{-13}, D_e(non): 5.58 x 10^{-9} m^2/s, r_o 25 x 10^{-6} m

For a similar diffusivity i.e., D_e(non): 5.58 x 10^{-9} m^2/s, the two Stremming isothermal and non-isothermal curves become equal. The Crank's uptake, although also increases, still slower than the Stremming curves.

The corresponding maximum uptakes at t = 0.01s are: 0.7436, 0.9999 and 0.9999 for Crank and Stremming isothermal and non-isothermal uptake curves respectively.

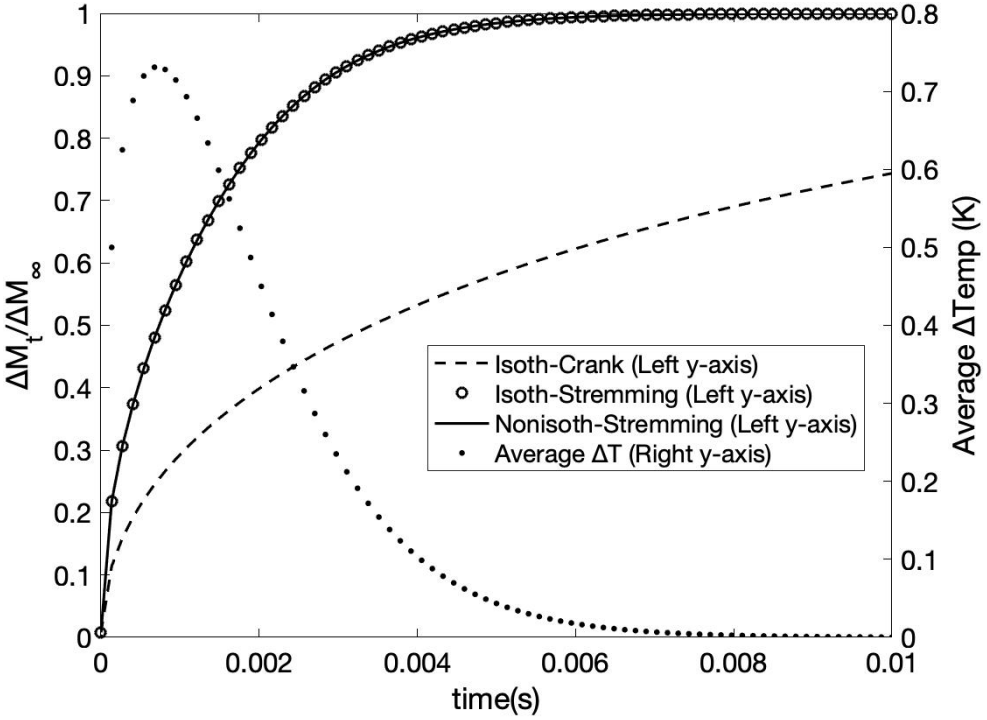

Figure 2.13: Isothermal and Non-isothermal Uptakes:D_e(non):5.58x$10^{-9}$$m^2$/s,$r_o$=25x$10^{-6}$m

2.4.2 *Effect of ΔH on Uptakes and $\overline{\Delta T}$*

Keeping the particle radius and diffusivities constant, the effect of heat of adsorption was studied and the results are shown in the table and plots below.

Table 2.8: Effect of ΔH on Uptake & $\overline{\Delta T}$:D_e(non)=5.58x10^{-9}m^2/s,r_o25x10^{-6}m

ΔH (J/mol)	Max. $\Delta M_t/\Delta M_\infty$	Max. $\overline{\Delta T}$
34.1 x 10^4	0.9999	7.2577
84.1 x 10^4	0.9999	17.8235
134.1 x 10^4	0.9999	28.3002
184.1 x 10^4	0.9999	38.6892

From the plots and table below, it is quite clear varying ΔH barely affects the CO_2 uptake curves. This is mainly because the model was derived on the assumption that D_e is independent of temperature; and partly due to the micro size of the MOF-5 particle. The model gives indifferent uptake curves for the increasing heats of adsorption. However, for the same adsorption process heats of adsorption, the $\overline{\Delta T}$ profiles are significantly distinct. This gives an insight the model is partly correctly applicable for this analysis.

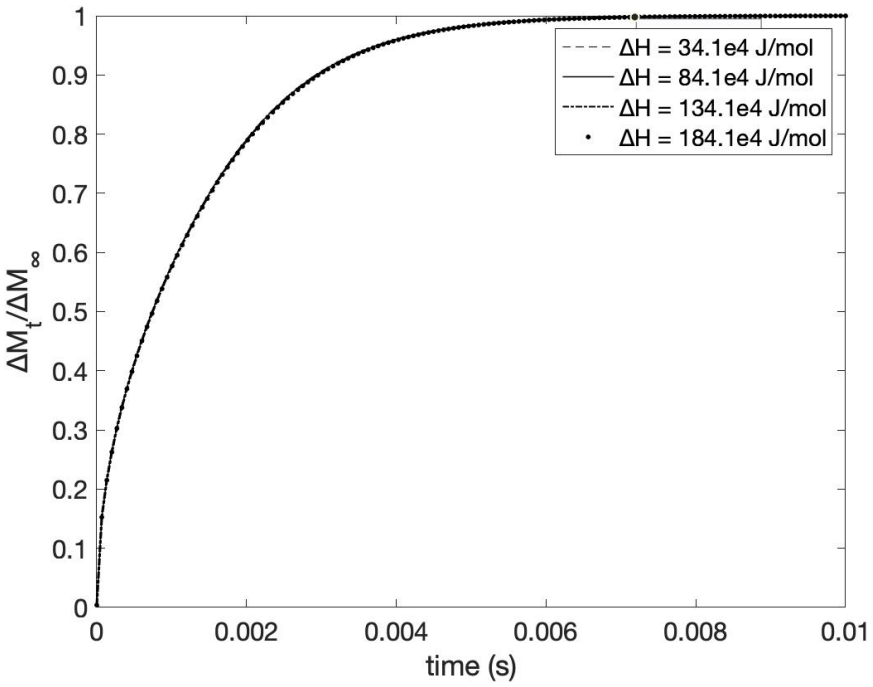

Figure 2.14: Effect of ΔH on Uptakes: D_e(non): 5.58 x 10^{-9} m^2/s, r_o 25 x 10^{-6} m

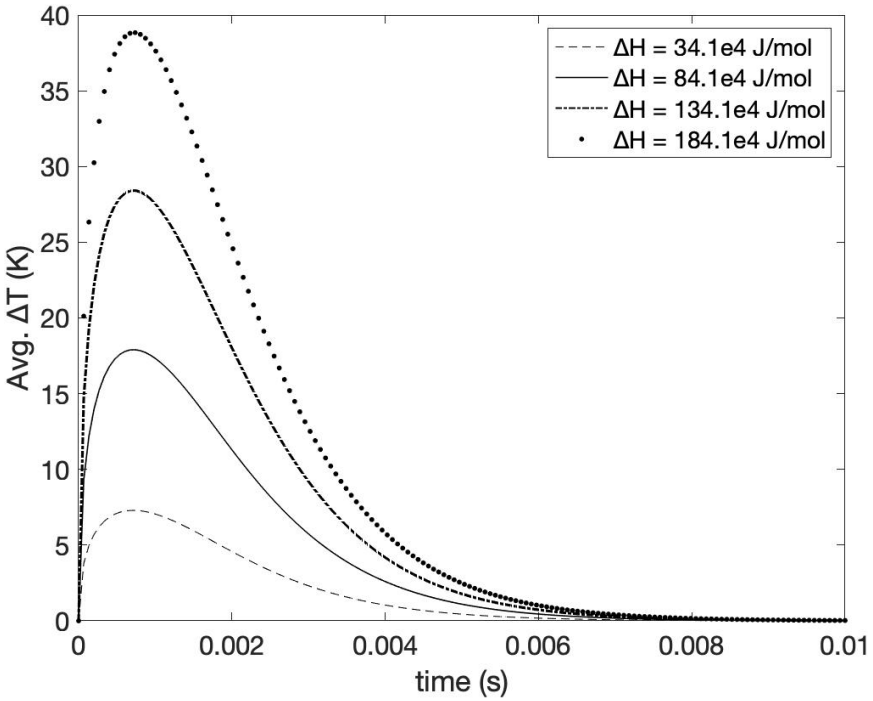

Figure 2.15: Effect of ΔH on $\overline{\Delta T}$: D_e(non): 5.58 x 10^{-9} m^2/s, r_o 25 x 10^{-6} m

2.4.3 *Effect of Particle Radius, r_0, on Uptake and $\overline{\Delta T}$*

For ΔH = 34.1 x 10^4 J/mol and D_e(non) = 5.58 x 10^{-10} m^2/s, the effect of particle size is seen to follow a similar trend as seen for the benzene-silica gel case. As already seen, maximum CO_2 uptake and $\overline{\Delta T}$ reduce with increasing particle size.

The model is adequate for the analysis of the effect of particle radius on sorbate uptake and average temperature differences, but more sufficient for larger particles, for which the adsorption takes significant time to reach equilibrium.

Table 2.9: Effect of r_0 on Uptake & $\overline{\Delta T}$:D_e=5.58x$10^{-10}$$m^2/s$,$\Delta H$=34.1x$10^4$J/mol,t=0.1s

r_0 (m)	Max. $\Delta M_t/\Delta M_\infty$	Max. $\overline{\Delta T}$
25 x 10^{-6}	1.000	2.2997
25 x 10^{-5}	0.3189	2.0516
25 x 10^{-4}	0.0319	0.2974

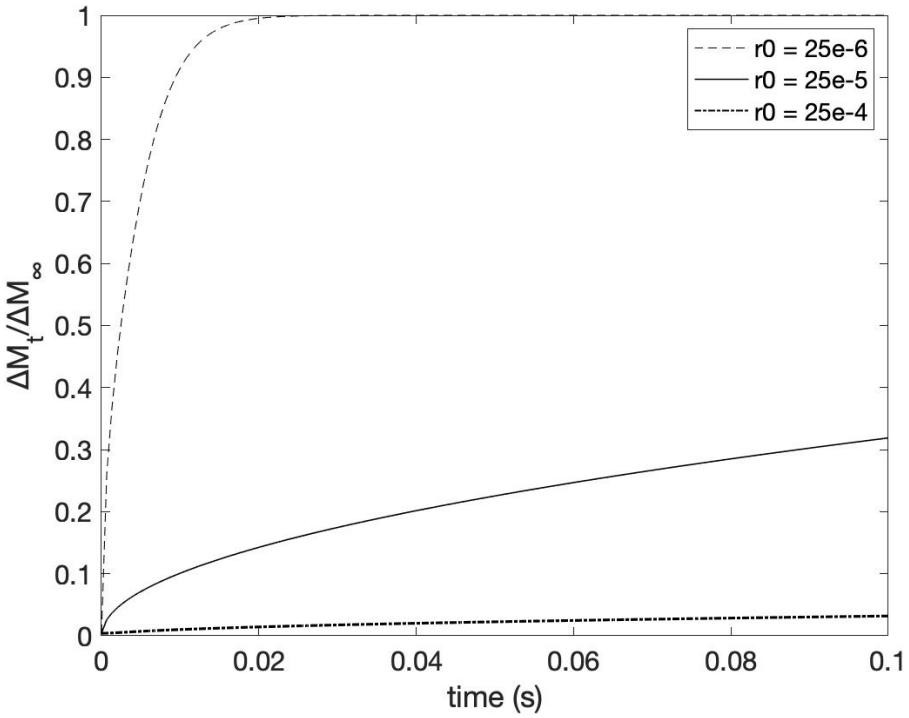

Figure 2.16: Effect of r_0 on $\overline{\Delta T}$:D_e=5.58x 10^{-10}m^2/s, ΔH=34.1x10^4 J/mol, t = 0.1s

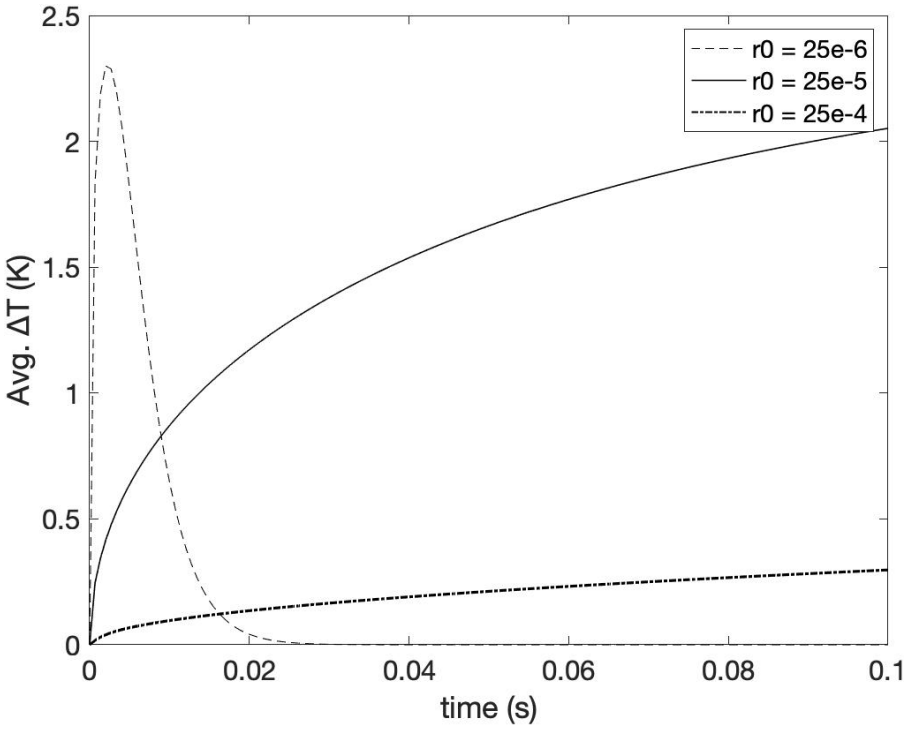

Figure 2.17: Effect of r_0 on $\overline{\Delta T}$:D_e=5.58x10^{-10}m^2/s,ΔH=34.1x10^4J/mol, t=0.1s

2.4.4 Effect of Diffusivity, D_e, on Uptake and $\overline{\Delta T}$

For r_0 = 25 x 10^{-6} m and ΔH = 34.1 x 10^4 J/mol, the maximum uptake of CO_2 on MOF-5 at t = 0.01s increases with increasing diffusivity, D_e, and so does the average temperature difference. The higher the diffusivity, the faster the CO_2 diffusion in the MOF-5 porous network, and thus faster uptake. The average temperature difference in the MOF-5 particle ultimately increases due to increasing kinetic energy as a result of rapid movement of CO_2 molecules. For small diffusivities, $\overline{\Delta T}$ values are small; likely due to the reduced mobility of the CO_2 molecules through the MOF-5 particle, which reduces diffusion, and thus low kinetic energy of CO_2 molecules, leading to slower uptake curves.

Table 2.10: Effect of D_e on Uptake & $\overline{\Delta T}$: ΔH=34.1x10^4J/mol,r_0=25x10^{-6}m,t=0.01s

D_e (m^2/s)	Max. $\Delta M_t/\Delta M_\infty$	Max. $\overline{\Delta T}$
5.58 x 10^{-10}	0.9148	2.3063
5.58 x 10^{-9}	0.9999	7.2910
5.58 x 10^{-8}	1.000	22.9974

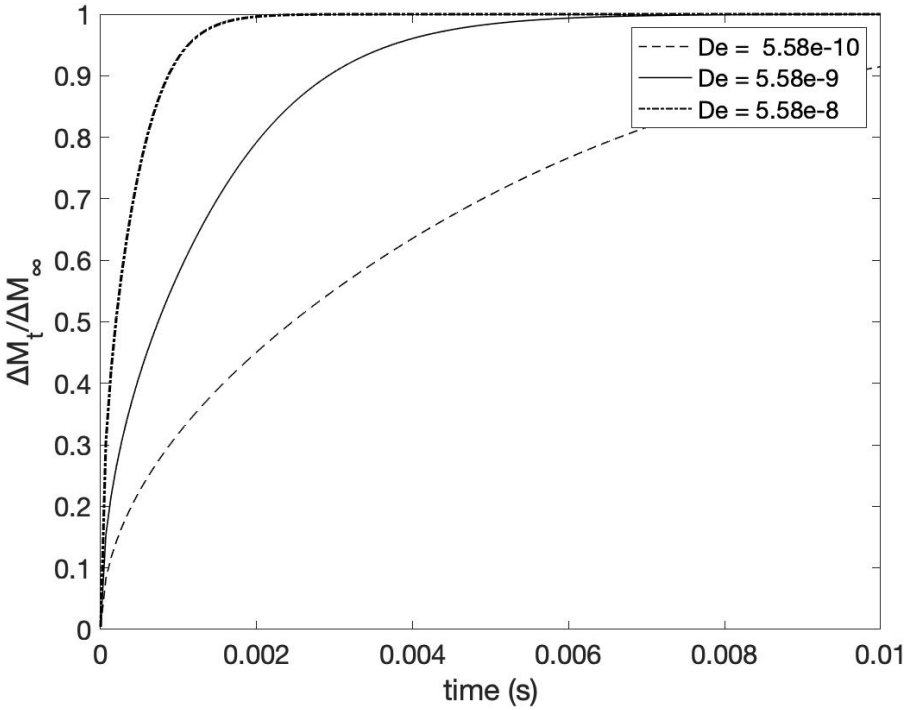

Figure 2.18: Effect of D_e on Uptake: ΔH=34.1x10^4 J/mol, r_0=25x10^{-6}m, t=0.01s

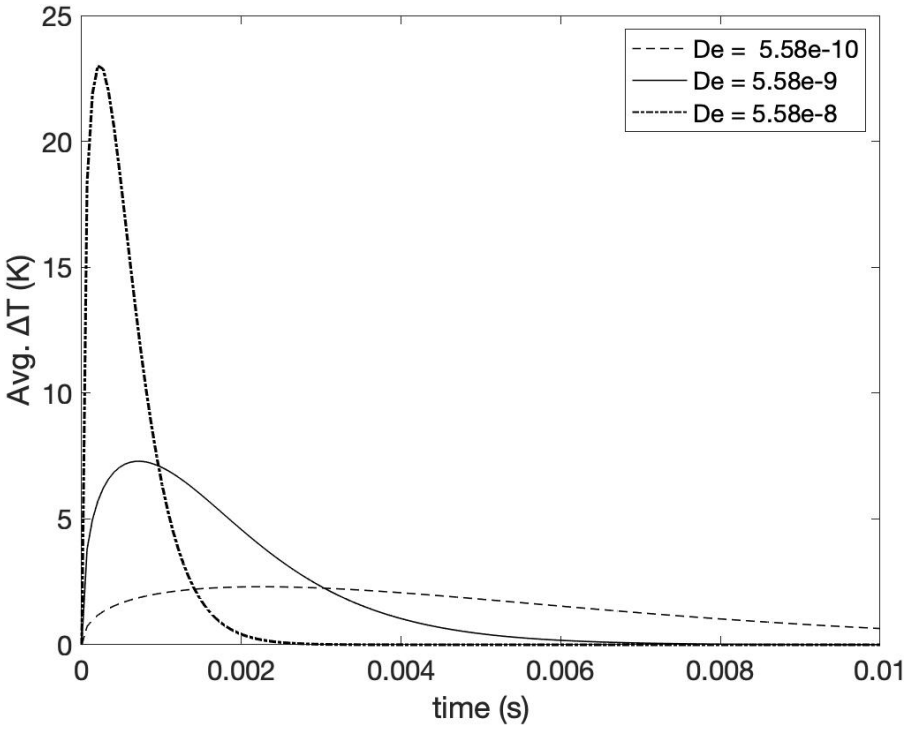

Figure 2.19: Effect of D_e on $\overline{\Delta T}$: ΔH=34.1x10^4J/mol, r_0=25x10^{-6}m, t=0.01s

2.5 Conclusions

Isothermal models are only adequate for the determination of the extent of adsorbate uptakes in porous particles. The increase in the average particle temperature as a result of the heat generated during adsorption is overlooked.

The Stremming non-isothermal model, while sufficient for the benzene and the mesoporous silica gel adsorption process, is not thoroughgoing for microporous adsorbents such as MOF-5. The 0.7K maximum change in average particle temperature calculated using this non-isothermal model for the CO_2 adsorption on a MOF-5 particle gives an impression that the adsorption is rather isothermal, which is actually not.

The following chapter introduces a new model used for the analysis of this adsorption.

Chapter 3

ANALYSIS OF CO_2 ADSORPTION ON MOF-5 USING NEW MODEL

3.1 Basis

Although it considers a finite effective thermal conductivity, *Haul & Stremming* model described above is ideally sufficient for the analysis of adsorption in mesoporous adsorbents i.e., adsorbent particles whose pore sizes are between 2 and 50 nm[21]. For such particles, pores are large enough to accommodate both the adsorbed and vapor phases during adsorption. In other words, some adsorbate molecules are adsorbed on the pore walls (adsorbed phase), while the rest are in motion through the particle pore network (vapor phase).

For microporous adsorbents, like zeolites and MOF-5, whose particles have pores of size less than 2 nm,[3], the vapor phase concentration is too insignificant to assume in the analysis. Only the adsorbed phase concentration is appreciably high enough.

In addition, the CO_2 molecule is significantly large, with a 0.33 nm *kinetic* diameter[13] relative to adsorbent pore sizes. For instance, a MOF-5 particle has a pore size of 0.8 nm [30]. Basic arithmetic indicates there's hardly enough volume in the pore network to allow for the vapor phase.

The new analysis presented here not only assumes a finite thermal conductivity, but also takes into account the small pore size of a MOF-5 particle—and considers only the adsorbed phase to exhibit significant adsorbate (CO_2) concentration. Moreover, the non-isothermal adsorption models that assume finite adsorbent thermal conductivities are constrained by the assumption of

constant diffusivity of the adsorbate in the adsorbent during the process, which this model addresses.

3.2 The New Model

The non-isothermal diffusion of CO_2 in a MOF-5 particle is modeled as follows:

Mass Balance:

$$\frac{\partial q}{\partial t} \;=\; \frac{1}{r^2}\,\frac{\partial}{\partial r}\left(D\,r^2\,\frac{\partial q}{\partial r}\right) \tag{3.1}$$

where,

$$D \;=\; D_0\,exp\left(-\frac{Ea}{RT}\right) \tag{3.2}$$

with the following initial and boundary conditions:

$$q\,(r,0) \;=\; 0\;, \qquad \left(\frac{\partial q}{\partial r}\right)_{r=0} \;=\; 0, \qquad q\,(r_0,t) \;=\; q_\infty$$

The heat changes that occur during adsorption contribute to the temperature changes. The corresponding heat balance is given as:

$$\rho\,c_p\frac{\partial T}{\partial t} \;=\; \frac{\lambda}{r^2}\,\frac{\partial}{\partial r}\left(r^2\,\frac{\partial T}{\partial r}\right) \;+\; \rho\,(-\Delta H)\,\frac{\partial q}{\partial t} \tag{3.3}$$

with initial and boundary conditions:

$$T\,(r,0) \;=\; T_0\;, \qquad \left(\frac{\partial T}{\partial r}\right)_{r=0} \;=\; 0, \qquad \left(\frac{\partial T}{\partial r}\right)_{r=r_0} \;=\; -\,\frac{h}{\lambda}\,(T-T_0),$$

in which q represents the adsorbed phase concentration of CO_2, D is the diffusivity, T is particle temperature, and r is the particle radius.

Equations (3.1) and (3.3) form a system of coupled of partial differential equations solved numerically after non-dimensionalization shown below.

Reduced Variables:

$$U_1 = \frac{q - q_0}{q_\infty - q_0}, \quad U_2 = \frac{T}{T_0}, \quad \tau = \frac{D_0\, t}{r_0^2}, \quad \eta = \frac{r}{r_0},$$

Dimensional Coefficients:

$$\alpha = \frac{\lambda}{\rho_0\, c_p}$$
$$\beta = \frac{(-\Delta H)}{c_p}$$

Dimensionless Variables:

$$Le = \frac{\alpha}{D_0}, \quad \theta = \frac{Ea}{R\,T_0}, \quad \phi = \frac{h\, r_0}{\lambda}, \quad \kappa = \frac{\beta\,(q_\infty\, -\, q_0)}{\rho_0\; T_0}, \quad \gamma = \frac{(-\Delta H)}{R\,T_0}$$

Upon simple, yet necessary substitutions and derivatives, equation (3.1) becomes:

$$\frac{\partial U_1}{\partial \tau} \;=\; exp\left(-\frac{\theta}{U_2}\right)\frac{\partial^2 U_1}{\partial \eta^2} \;+\; exp\left(-\frac{\theta}{U_2}\right)\left(\frac{2}{\eta} \;-\; \frac{\theta}{U_2^2}\,\frac{\partial U_2}{\partial \eta}\right)\frac{\partial U_1}{\partial \eta} \qquad (3.4)$$

with:

$$U_1\,(\eta, 0) \;=\; 0\;, \qquad \frac{\partial U_1}{\partial \eta}(0, \tau) = \;0, \qquad U_1\,(1, \tau) \;=\; 1$$

and equation (3.3) becomes:

$$\frac{\partial U_2}{\partial \tau} \;= Le\,\frac{\partial^2 U_2}{\partial \eta^2} \;+\; \kappa\, exp\left(-\frac{\theta}{U_2}\right)\frac{\partial^2 U_1}{\partial \eta^2} \;+\frac{2\,Le}{\eta}\frac{\partial U_2}{\partial \eta} +\;\; \kappa\, exp\left(-\frac{\theta}{U_2}\right)\left(\frac{2}{\eta} \;-\; \frac{\theta}{U_2^2}\,\frac{\partial U_2}{\partial \eta}\right)\frac{\partial U_1}{\partial \eta} \qquad (3.5)$$

and the corresponding initial and boundary conditions are:

$$U_2\,(\eta, 0) \;=\; 1\;, \qquad \frac{\partial U_2}{\partial \eta}(0, \tau) = \;0, \qquad U_2\,(1, \tau) \;=\; \phi\,(1 - U_2)$$

The system of coupled partial differential equations is solved using finite difference method (FDM), and MATLAB *pdepe* function. This process is detailed in the Appendix.

The models are tested using the experiment carried out by Zhao[31]. Firstly, the analyses are done using the Crank's and the derived isothermal models, and results are compared with *Haul* & *Stremming*'s non-isothermal model along with the corresponding average temperature differences, using the original diffusivity and the modified diffusivity, for both short (0.01 s) and long (10 s) times. A summary of the parameters and values used in this analysis is presented in the Appendix. The same experiment is subject to a similar analysis using the new presented model above. Results are reported in the following chapter.

3.3 Results for CO_2 - MOF-5 Adsorption Using New Model

Using the parameters used in Table A.11 (in the Appendix section), the model above is used to analyze CO_2 adsorption on MOF-5, and solved in MATLAB. In 10 seconds, the adsorbate concentration in the particle increases to the maximum value, at which point the reduced concentration U_1 is 1, as shown in Figure 5.20 below. Sample reduced concentration values are reported in Table A.12. The reduced particle temperature increases in the first few seconds of the process, and then settles to the initial (ambient) temperature as shown in Figure 5.21.

Numerical integration of U_1 values with respect to the radius gives the average reduced concentration in the particle with rest to reduced time. The same applies to the reduced temperature values. Upon integration of U_2, the average

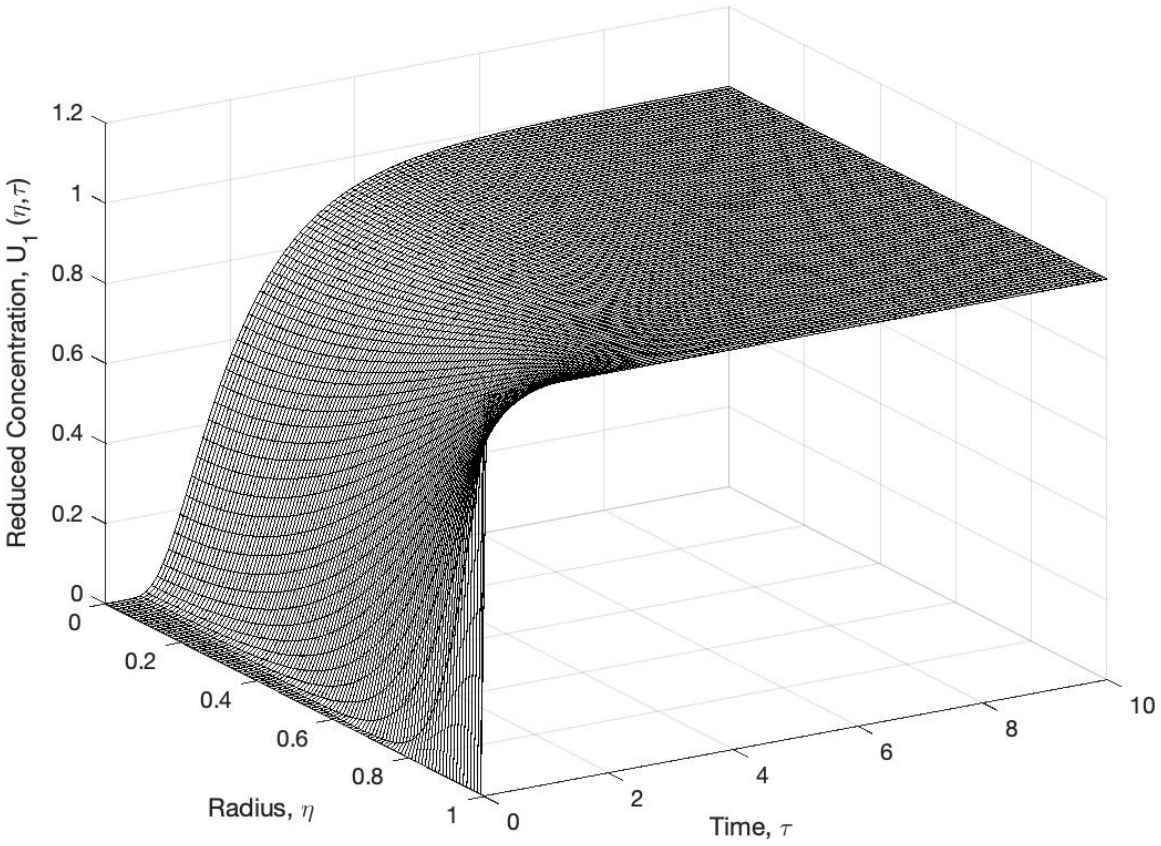

Figure 3.1: Reduced CO_2 Concentration in Particle, as a function of η and τ

reduced particle temperature is obtained, and shown in Table A.14.

The resulting plots of time-dependent reduced concentration and particle temperature are showed in Figures 5.22 and 5.23 respectively.

The maximum reduced temperature is roughly 1.02 which corresponds to 301 K, depicted in Figure 5.24.

The relative diffusivity values, of which the highest is 1.72 x 10^{-11} (m^2/s), are reported in the Table A.14.

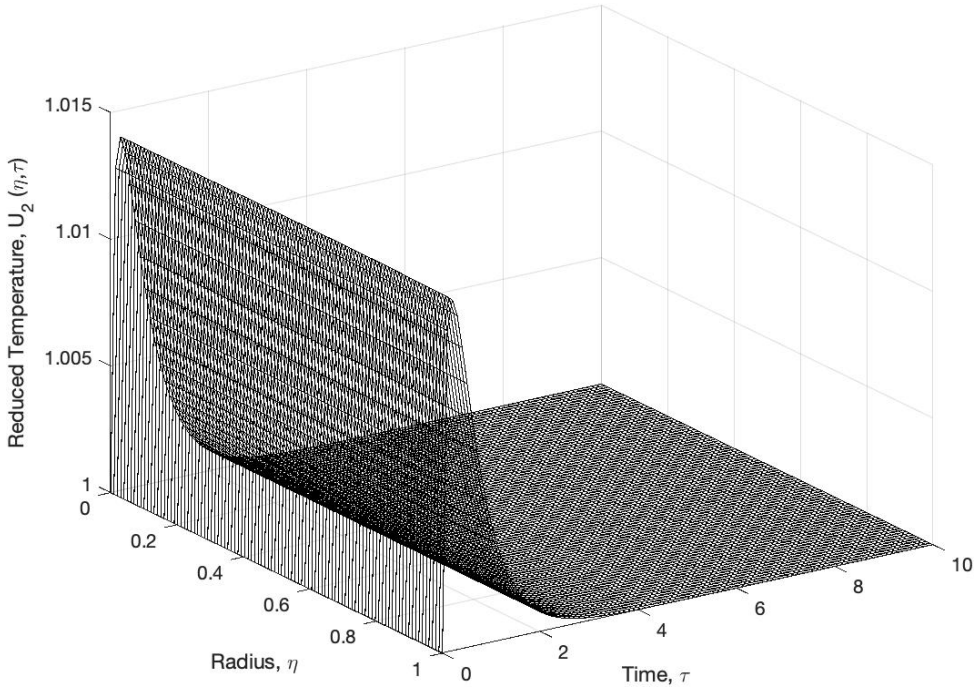

Figure 3.2: Reduced MOF-5 Particle Temperature, as a function of η and τ

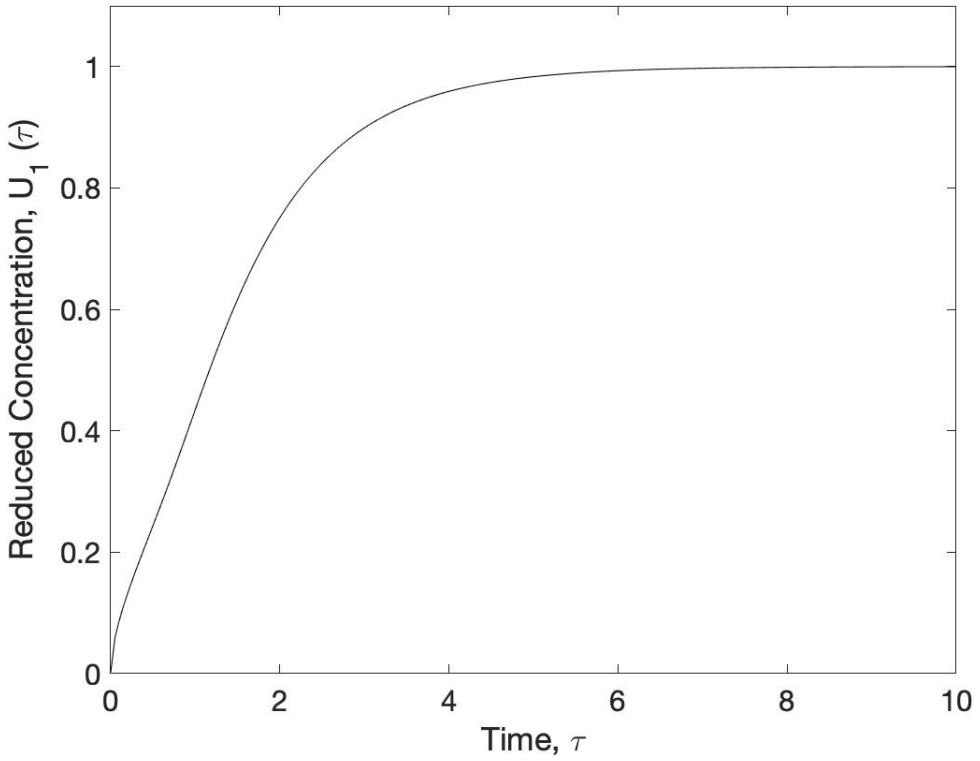

Figure 3.3: Reduced CO_2 Concentration as a function of τ

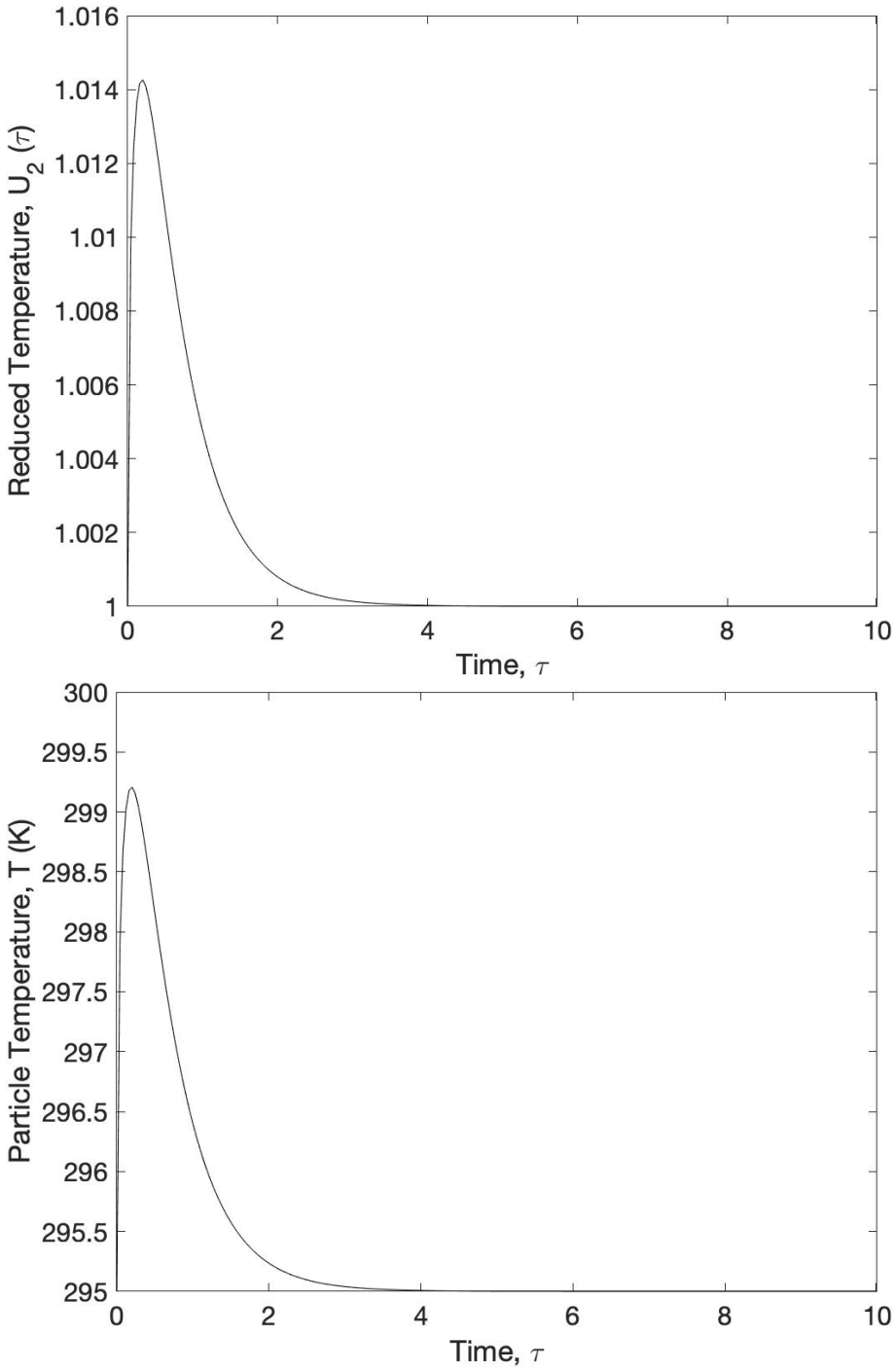

Figure 3.4: Reduced (top), and Average Particle Temperature (bottom)

3.4 Parametric Analyses

3.4.1 Effect of ΔH on CO_2 Uptake and Particle Temperature

From the plots below, there is no significant effect of heat of adsorption for r_0 = 25 x 10^{-6} m, T_0 =295 K, and effective thermal conductivity, λ = 0.0854 W/mK. However, particle temperature increases with increasing ΔH.

CO_2 uptake is influenced majorly by how much the ambient temperature is, by the particle temperature increase; of which the effect of the latter is only slightly significant since the temperature rise is seen as adsorption is occurring.

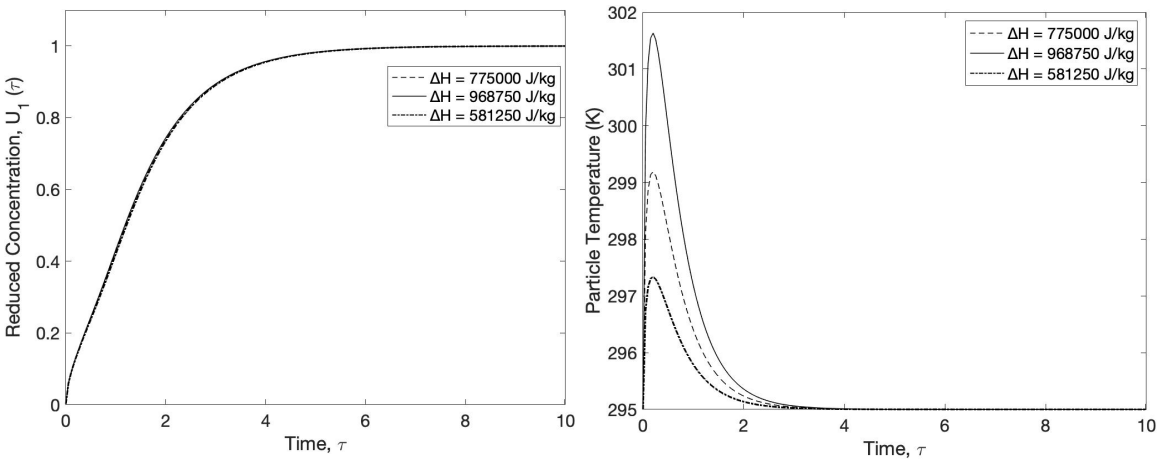

Figure 3.5: Effect of ΔH on CO_2 Uptake and Particle Temperature

3.4.2 Effect of r_0 on CO_2 Uptake and Particle Temperature

The particle radius affects both the amount of CO_2 adsorbed into the MOF-5 particle and the average particle temperature. Smaller particles exhibit a much rapid CO_2 uptake, and a higher maximum average particle temperature (302.89 K) as seen in Figure 3.6(e) and (f) respectively. Conversely, for larger particles,

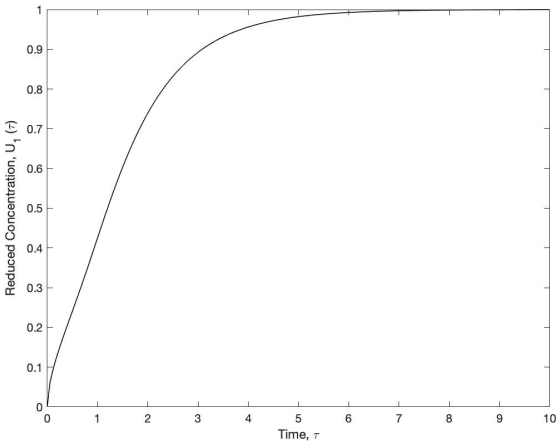

(a) $r_0 = 2.5$ x 10^{-5} m, time = 2.125 hours

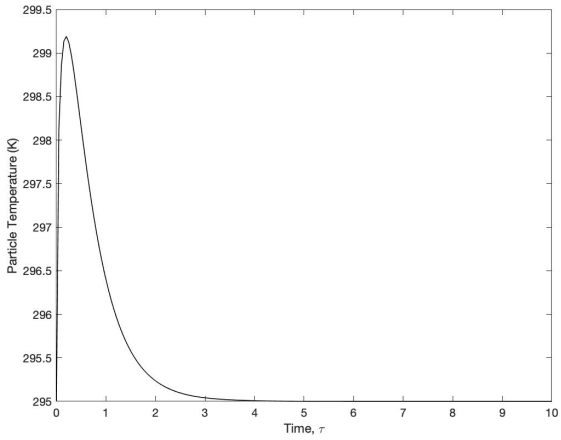

(b) $r_0 = 2.5$ x 10^{-5} m, time = 2.125 hours

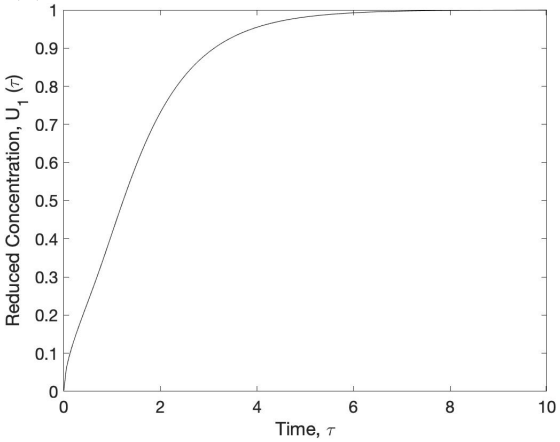

(c) $r_0 = 2.5$ x 10^{-4} m, time = 212.5 hours

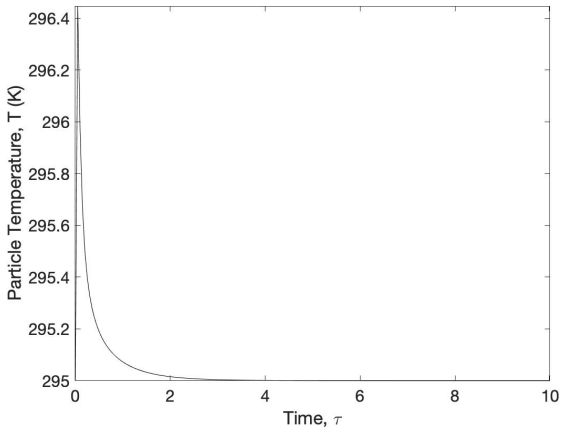

(d) $r_0 = 2.5$ x 10^{-4} m, time = 212.5 hours

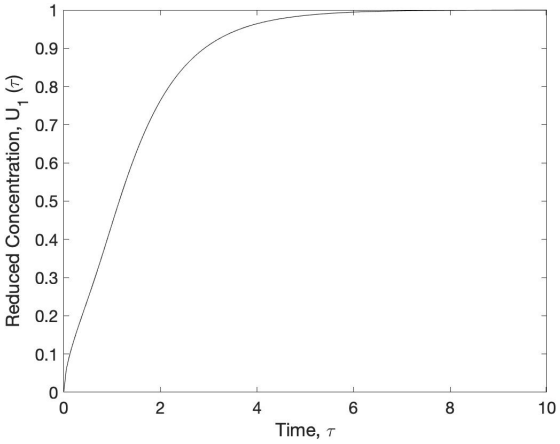

(e) $r_0 = 2.5$ x 10^{-6} m, time = 0.02125 hours

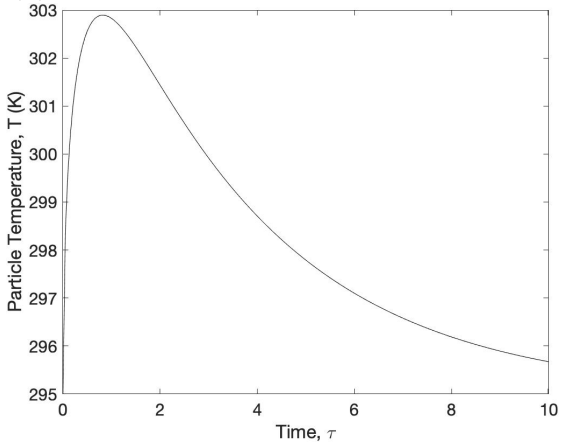

(f) $r_0 = 2.5$ x 10^{-6} m, time = 0.02125 hours

Figure 3.6: Effect of r_0 on CO_2 Uptake and Particle Temperature

uptake curve takes the longest to reach equilibrium CO_2 concentration in the particle; with the a lower maximum average particle temperature (296.45 K), seen in Figure 3.6(c) and (d). Plots in (a) and (b) are for the base/nominal case. Unlike for small particles, temperature in larger particles is distributed over a wide volume, and at any instant, the average temperature in the particle is significantly lower than in a small particle.

It is important to notice this analysis was done for the different times as indicated in the sub-plot captions, although the reduced times, τ, are scaled uniformly. See reduced variables definitions on page 49.

3.4.3 Effect of λ on CO_2 Uptake and Particle Temperature

There is no significant effect of the effective thermal conductivity on the CO_2 concentration in the particle. Particle temperature, however, increases with λ, as expected.

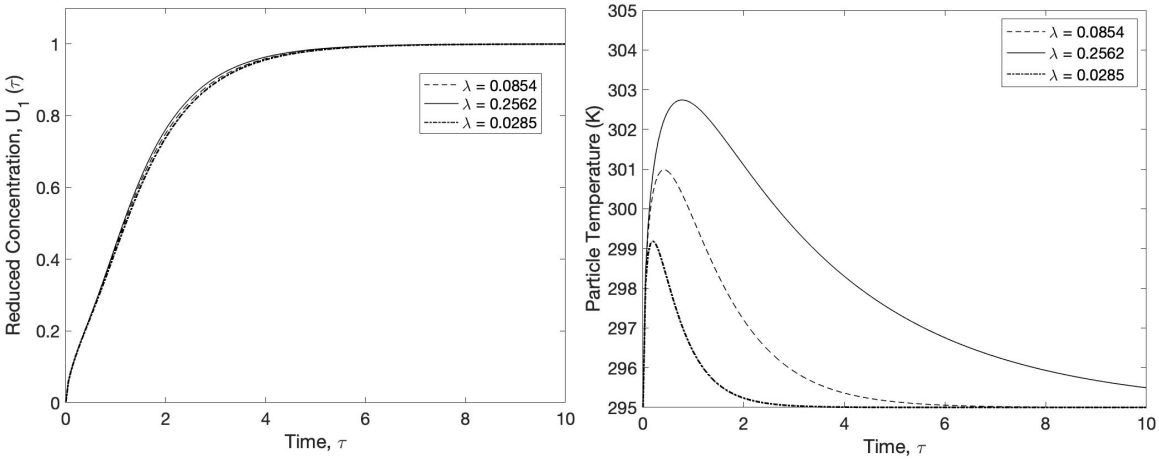

Figure 3.7: Effect of λ on CO_2 Uptake and Particle Temperature

3.4.4 *Effect of Temperature on CO_2 Uptake and Particle Temperature*

To understand the effect of temperature of the CO_2 sorption, an isothermal case was considered by making $\Delta H = 0$, at different ambient temperatures.

Results show that at higher temperatures, CO_2 uptake is more rapid than at lower temperatures. For instance, the uptake curve at 355 K as seen in Figure 3.8 is much steeper than that at 150 K. This is because at high temperatures, CO_2 molecules possess high enough kinetic energy to enable their diffusion into the pore network of the adsorbent particle. Ambient temperature is unchanged.

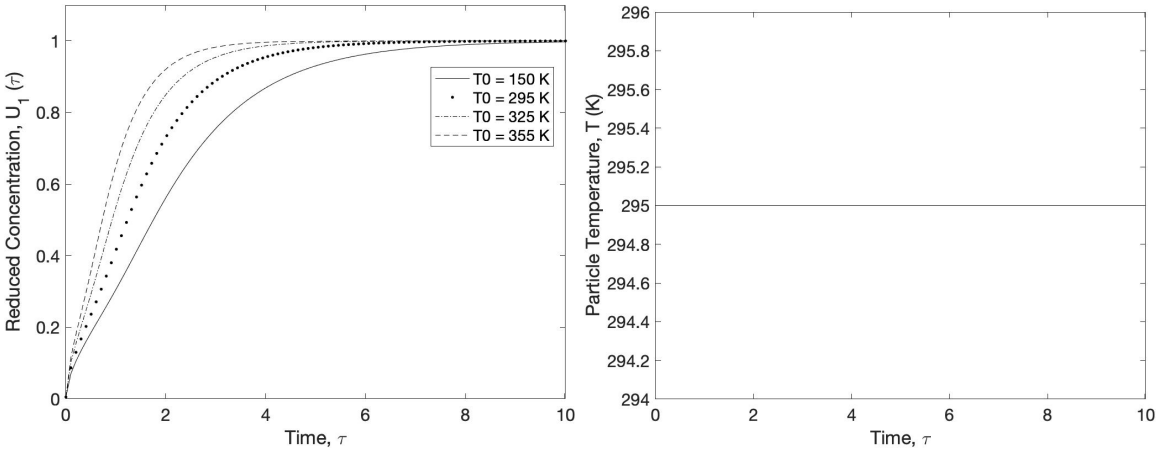

Figure 3.8: Effect of Temperature on CO_2 Uptake and Particle Temperature

3.5 Conclusion

The new model adequately analyzes the non-isothermal adsorption of CO_2 on the microporus MOF-5 particle. The heat generated during the process causes a significant 6K average particle temperature rise from the ambient temperature, as seen Figure 3.4.

For larger heats of adsorption, the average particle temperature increases appreciably; giving an impression that isothermal models are flawed for the analysis of this adsorption, like in Figure 3.5.

Smaller particles show a much larger average temperature in the particle than particles with bigger radii.

Chapter 4

SUMMARY AND RECOMMENDATION FOR FUTURE WORK

The Stremming non-isothermal and derived isothermal models can be applied to analyze adsorption of CO_2 on MOF-5 particles, as well as benzene on silica gel.

From the analysis, however, ignoring the heat effects of adsorption ultimately lead to misleading and inaccurate diffusivities. When isothermal adsorption is assumed, the resulting diffusivities are lower than those obtained for non-isothermal adsorption. The diffusivities for non-isothermal cases are higher, which quickens the process.

For the case of CO_2 adsorption on MOF-5, for example, the isothermal adsorption diffusivity initially calculated was 8.17 x 10^{-13} m^2/s, yet after an analysis considering non-isothermal adsorption, D_e is 5.58 x 10^{-13} m^2/s.

However, it was noticed the Stremming non-isothermal model is not the most adequate for the analysis of this adsorption process. It shows little to no effect of heat of adsorption on the uptakes; principally because the model was derived on the assumption that D_e does not depend on temperature, thus ΔH (and average temperature increments in the particle) don't influence the amount of adsorbate adsorbed.

When the new model, suitable for analysis of adsorption in microporous particles, is used for the analysis of CO_2 adsorption on a MOF-5 particle, the resultant particle temperature changes are observed. The difference between ambient temperature and the highest particle temperature during the process is

quite small, ≈ 6 K. In some adsorption processes, this small temperature change would qualify the process as isothermal. However, under some process conditions, the particle temperatures are significantly high, and the non-isothermal assumption is validated. For instance, from above, for ΔH increased by 1.25 times to 968750 J/kg, $\Delta T \approx 9.5$ K, which is a significant difference. Since there's uptake is barely affected, it may be conjectured that the temperature increase only facilitates the intraparticle diffusion of CO_2 molecules, rather than its diffusion into the MOF-5 particle.

Particle radius affects both the uptake and temperature i.e., for smaller particles, i.e., $r_0 = 25 \text{ x } 10^{-6}$ m, the ΔT is well over 4 K.

As a result of the temperature change, the diffusivity increases from $8.17 \text{ x } 10^{-13}$ to $1.72 \text{ x } 10^{-11}$ m^2/s and falls back to the initial value rapidly, as seen in the Appendix.

For future work, this study may be stretched to analyze adsorption in a fixed-bed adsorber. Mass and heat balances for adsorbed phases and vapor phases through the bed voidage network, density of the bed, bed diameter, pressure drop etc, need to be taken into account in the analysis. Also, an experimental determination of the diffusivity changes during this non-isothermal adsorption would be another frontier to explore.

REFERENCES

[1] Admin. Adsorption - definition, applications, types of adsorption, isotherm.

[2] Admin. Chemisorption, particle technology labs.

[3] Arpita Hazra Chowdhury, Noor Salam, Rinku Debnath, Sk Manirul Islam, and Tanima Saha. Design and fabrication of porous nanostructures and their applications. In *Nanomaterials Synthesis*, pages 265–294. Elsevier, 2019.

[4] John Crank. *The mathematics of diffusion*. Oxford university press, 1979.

[5] Richard P Gangloff and Brian P Somerday. *Gaseous hydrogen embrittlement of materials in energy technologies: the problem, its characterisation and effects on particular alloy classes*. Elsevier, 2012.

[6] CJ Geankoplis. Transport processes and separation process principles (includes unit operations). In *Process Principles*. Prentice Hall NJ, 2003.

[7] R Haul and H Stremming. Nonisothermal sorption kinetics in porous adsorbents. *Journal of colloid and interface science*, 97(2):348–355, 1984.

[8] BL Huang, Z Ni, A Millward, AJH McGaughey, C Uher, M Kaviany, and O Yaghi. Thermal conductivity of a metal-organic framework (mof-5): Part ii. measurement. *International Journal of Heat and Mass Transfer*, 50(3-4):405–411, 2007.

[9] Vassilis Inglezakis and Stavros Poulopoulos. *Adsorption, ion exchange and catalysis*, volume 3. Elsevier, 2006.

[10] Hellmut G Karge and Jens Weitkamp. *Adsorption and diffusion*, volume 7. Springer Science & Business Media, 2008.

[11] FA Kloutse, R Zacharia, D Cossement, and R Chahine. Specific heat capacities of mof-5, cu-btc, fe-btc, mof-177 and mil-53 (al) over wide temperature ranges: Measurements and application of empirical group contribution method. *Microporous and Mesoporous Materials*, 217:1–5, 2015.

[12] Lap-Keung Lee and Douglas M Ruthven. Analysis of thermal effects in adsorption rate measurements. *Journal of the Chemical Society, Faraday Transactions 1: Physical Chemistry in Condensed Phases*, 75:2406–2422, 1979.

[13] Xue Li, Wenhao He, Xiaonan Hou, Li Zhao, Ge Zhao, Guiwu Lu, and Junqing Chen. Study on co_2 adsorption and permeance of porous carbon and nitrogen membranes co-regulated by charge and strain. In *Journal of Physics: Conference Series*, volume 2168, page 012002. IOP Publishing, 2022.

[14] James Clerk Maxwell. Iv. on the dynamical theory of gases. *Philosophical transactions of the Royal Society of London*, (157):49–88, 1867.

[15] Ludovic Montastruc, Pascal Floquet, Volker Mayer, Iordan Nikov, and Serge Domenech. Kinetic modeling of isothermal or non-isothermal adsorption in a pellet: Application to adsorption heat pumps. *Chinese Journal of Chemical Engineering*, 18(4):544–553, 2010.

[16] Roger Nix. Kinetics of adsorption. 2022.

[17] Justin Purewal, Dongan Liu, Andrea Sudik, Mike Veenstra, Jun Yang, Stefan Maurer, Ulrich Muller, and Donald J Siegel. Improved hydrogen storage and thermal conductivity in high-density mof-5 composites. *The Journal of Physical Chemistry C*, 116(38):20199–20212, 2012.

[18] Suprakas Sinha Ray, Rashi Gusain, and Neeraj Kumar. *Carbon nanomaterial-based adsorbents for water purification: Fundamentals and applications*. Elsevier, 2020.

[19] DM Ruthven. Physical adsorption and the characterization of porous adsorbents. *Principles of adsorption and adsorption processes*, 19, 1984.

[20] Douglas M Ruthven, Lap-Keung Lee, and Hayrettin Yucel. Kinetics of nonisothermal sorption in molecular sieve crystals. *AIChE Journal*, 26(1):16–23, 1980.

[21] Tawfik A Saleh. Properties of nanoadsorbents and adsorption mechanisms. In *Interface Science and Technology*, volume 34, pages 233–263. Elsevier, 2022.

[22] Seetharaman Sridhar. A commentary on "diffusion, mobility and their interrelation through free energy in binary metallic systems," ls darken: Trans. aime, 1948, vol. 175, p. 184ff. *Metallurgical and Materials Transactions A*, 41:543–562, 2010.

[23] LM Sun and F Meunier. A detailed model for nonisothermal sorption in porous adsorbents. *Chemical engineering science*, 42(7):1585–1593, 1987.

[24] Chi Tien. *Introduction to adsorption: Basics, analysis, and applications*. Elsevier, 2018.

[25] Chi Tien. *Introduction to adsorption: Basics, analysis, and applications*. Elsevier, 2018.

[26] Kai Trepte and Sebastian Schwalbe. Systematic analysis of porosities in metal-organic frameworks. 2020.

[27] Cheng-Si Tsao, Ming-Sheng Yu, Tsui-Yun Chung, Hsiu-Chu Wu, Cheng-Yu Wang, Kuei-Sen Chang, and Hsin-Lung Chen. Characterization of pore structure in metal- organic framework by small-angle x-ray scattering. *Journal of the American Chemical Society*, 129(51):15997–16004, 2007.

[28] Ohio University. Properties of various ideal gases (at 300 k). Accessed October 16, 2022.

[29] Amrita Vishwa vidyapeetham virtual lab. Adsorption isotherm (theory)physical chemistry virtual lab. Accessed September 10, 2022.

[30] Jiashu Yuan, Cuijuan Zhang, Qianyuan Qiu, Zheng-Ze Pan, Lijun Fan, Yicheng Zhao, and Yongdan Li. Highly selective metal-organic framework-based (mof-5) separator for non-aqueous redox flow battery. *Chemical Engineering Journal*, 433:133564, 2022.

[31] Zhenxia Zhao, Zhong Li, and YS Lin. Adsorption and diffusion of carbon dioxide on metal- organic framework (mof-5). *Industrial & Engineering Chemistry Research*, 48(22):10015–10020, 2009.

APPENDIX A

MATLAB PDEPE FORMULATION

Parameters used in the calculations are given in Table A.11.
The pdepe solver is given as follows.

$$c\left(x,t,u,\frac{\partial u}{\partial x}\right)\frac{\partial u}{\partial t}=\frac{1}{x^m}\frac{\partial}{\partial x}\left(x^m\, f(x,t,u,\frac{\partial u}{\partial x})\right)+s\left(x,t,u,\frac{\partial u}{\partial x}\right) \qquad \text{(A.1)}$$

From the given system of coupled pdes, in equation (3.4) and (3.5),

$$c = \begin{bmatrix}1\\1\end{bmatrix}$$

$$f = \begin{bmatrix} exp\left(-\frac{\theta}{U_2}\right)\frac{\partial U_1}{\partial \eta} \\ Le\,\frac{\partial U_2}{\partial \eta} + \kappa\, exp\left(-\frac{\theta}{U_2}\right)\frac{\partial U_1}{\partial \eta}\end{bmatrix}$$

$$s = \begin{bmatrix} exp\left(-\frac{\theta}{U_2}\right)\left(\frac{2}{\eta} - \frac{\theta}{U_2^2}\frac{\partial U_2}{\partial \eta}\right)\frac{\partial U_1}{\partial \eta} \\ \frac{2\,Le}{\eta}\frac{\partial U_2}{\partial \eta} + \kappa\, exp\left(-\frac{\theta}{U_2}\right)\left(\frac{2}{\eta} - \frac{\theta}{U_2^2}\frac{\partial U_2}{\partial \eta}\right)\frac{\partial U_1}{\partial \eta}\end{bmatrix}$$

$m = 0$

U_1 represents CO_2 concentration
U_2 represents particle temperature
x represents η

Chapter B

MATLAB CODE

```
D0 = 8.17e-13; % m2/s
Ea =7.61e3; % J/mol
R = 8.314; % J/mol K
H = 0;%7.75e5;
%H = 968750; % J/kg
%H = 581250; % J/kg
lambda = 0.0854; % W/m K
cp = 815; % J/kg K Effective heat capacity
rhoe = 130; % Density of porous  MOF
rho = 750; % Density of solid MOF
q_inf = 91.5842; % kg of CO2 per m3 of MOF
q0 = 0;  % kg of CO2 per m3 of MOF
T0 = 295.0; % K

r0 = 2.5e-5; % particle radius
%r0 = 2.5e-4;
%r0 = 2.5e-6;

time =  7650;  %process time (2.125 hours)
N = 200;  %Number of grid points
xmesh = linspace(0, 1, N); % Reduced radius r/r0=1
tmesh = linspace(0, time, N);
tau = D0*tmesh./(r0.^2); % Reduced time

sol = pdepe(2, @pdefun, @icfun, @bcfun, xmesh, tau);
U_1 = sol(:,:,1); % Reduced concentration as a
```

```
   function of both time and radius
U_2 = sol(:,:,2); % Reduced temperature as a function
   of both time and radius

surf(xmesh, tau, U_1,'FaceAlpha','0');
colormap([0  0  0])
%title('Reduced Concentration')
xlabel('Radius, \eta')
ylabel('Time, \tau')
zlabel('Reduced Concentration, U_1 (\eta,\tau)')

figure;
surf(xmesh, tau, U_2,'FaceAlpha','0');
%title('Reduced Temperature')
xlabel('Radius, \eta')
ylabel('Time, \tau')
zlabel('Reduced Temperature, U_2 (\eta,\tau)')

Q = trapz(xmesh,U_1,2); % CO2 concentration a fucntion
    of time
P = trapz(xmesh,U_2,2); % Reduced particle temperature
    a fucntion of time
P1 = 295*(P); % Particle temperature
D = D0*exp(Ea/(R*P1))'; % Diffusivity as a function of
    temperature.
```

```
plot(tau,Q,'k')
%title('Reduced Concentration')
xlabel('Time, \tau')
ylabel('Reduced Concentration, U_1 (\tau)')
set(gca,'FontSize',15)

plot(tau,P,'k')
%title('Reduced Temperature, U_2 (\tau)')
xlabel('Time, \tau')
ylabel('Reduced Temperature, U_2 (\tau)')
set(gca,'FontSize',15)

plot(tau,P1,'k')
%title('Reduced Temperature, U_2 (\tau)')
xlabel('Time, \tau')
ylabel('Particle Temperature, T (K)')
set(gca,'FontSize',15)

function [c, f, s] = pdefun(x, t, u, dudx)
D0 = 8.17e-13; % m2/s
Ea =7.61e3; % J/mol
R = 8.314; % J/mol K
H = 7.75e5; % J/kg
%H = 968750; % J/kg
%H = 581250; % J/kg
lambda = 0.0854; % W/m K
```

```
cp = 815; % J/kg K Effective heat capacity
rhoe = 130; % Density of porous  MOF
rho = 750; % Density of solid MOF
q_inf = 91.5842; % kg of CO2 per m3 of MOF
q0 = 0;  % kg of CO2 per m3 of MOF
T0 = 295.0; % K

alpha  =  lambda/((rho*cp));
beta  =  H/cp;
Le  =  alpha/D0;
kappa  =  (beta*(q_inf-q0 ))/T0;
theta = Ea/(R*T0);



    c = [1; 1];

    f = [(exp(-theta/(u(2))))*dudx(1)
        Le*dudx(2) + kappa*(exp(-theta/(u(2))))*dudx
           (1)];

    s = [(exp(-theta/(u(2))))*(((2/x)-theta/(u(2))^2*
       dudx(2))*dudx(1))
        (2*Le/x)*dudx(2) + kappa*((exp(-theta/(u(2))))
           *(2/x-theta/(u(2))^2*dudx(2))*dudx(1))];

end
```

```
function u0 = icfun(x)
    u0 = [0; 1]; % Initial conditions
end

function [pl, ql, pr, qr] = bcfun(xl, ul, xr, ur, t)
D0 = 8.17e-13; % m2/s
Ea =7.61e3; % J/mol
R = 8.314; % J/mol K
H = 7.75e5; % J/kg
%H = 968750; % J/kg
%H = 581250;

cp = 815; % J/kg K Effective heat capacity
rhoe = 130; % Density of porous  MOF
rho = 750; % Density of solid MOF
q_inf = 91.5842; % kg of CO2 per m3 of MOF
q0 = 0;  % kg of CO2 per m3 of MOF
T0 = 295.0;
p0 = 101325; % Pa
h = 649; % effective heat transfer coefficient

%lambda = 0.0854; % W/m K  Effective thermal
   conductivity of MOF-5
%lambda = 0.2562;
lambda = 0.0285;
```

```
r0 = 2.5e-5;  %m
%r0 = 2.5e-4; %m
%r0 = 2.5e-6; %m

gamma = H/(R*T0);
phi = (h*r0)/lambda;
% alpha  =  lambda/((rho*cp));
% beta  =  H/cp;
% Le  =  alpha/D0;
% kappa  =  (beta*(q_inf-q0 ))/T0;
% theta = Ea/(R*T0);
k0 = 2.5144e-15; % Adsorption constant at infinite
   dilution
% left boundary conditions
pl = [0; 0];
ql = [1; 1];
% right boundary conditions
pr = [ur(1)-1; -phi*(1-ur(2))];
qr = [0; 1];
end
```

Chapter C

PARAMETERS USED IN THE ANALYSES

Table C.1: Parameters for Adsorption of Benzene on Silica gel Particle

Parameter	Symbol	Value	Units
Porosity	ϵ	0.64	
Particle radius	r_0	2.5	mm
Density of silica gel framework	ρ_0	2.2	g/cm^3
Density of silica gel	ρ_ϵ	0.79	g/cm^3
Specific heat of silica gel	$c_s(SiO_2)$	0.75	J/g/K
Specific heat of liquid benzene	$c_s(C_6H_6)$	1.74	J/g/K
Effective thermal conductivity	λ	4 x 10^{-4}	J/cm/s/K
Thermal conductivity of gaseous benzene	λ_g	8.5 x 10^{-4}	J/cm/s/K
Conduction heat transfer coefficient	h(cond)	3 x 10^{-4}	J/cm^2/s/K
Radiation heat transfer coefficient	h(rad)	4 x 10^{-4}	J/cm^2/s/K
Effective heat transfer coefficient	h	7	J/cm^2/s/K
Boltzmann's constant	σ	5.78 x 10^{-12}	J/cm^2/s/K^4
Emissivity	$e_1 = e_2$	0.8	
Nusselt's number	Nu	2	
Temperature	T_0	298	K
Initial sorbate amount	M_0	0.45 x 10^{-3}	mole/g
Final sorbate amount	M_∞	0.53 x 10^{-3}	mole/g
Heat of adsorption	-ΔH	41.9	kJ/mol
Slope of adsorption isotherm	β	760	
Slope of adsorption isobar	α	1.3 x 10^{-5}	mole/cm^3/K

Values Extracted from Haul and Stremming Experiment.

Table C.2: Parameters for Adsorption of CO_2 on MOF-5

Parameter	Symbol	Value	Units
Porosity[26]	ϵ	0.772	
MOF-5 particle radius[31]	r_0	25	μm
Density of MOF-5 framework	ρ_0	0.75	g/cm^3
Density of MOF-5[17]	ρ_ϵ	0.13	g/cm^3
Total pore volume[31]	V_p	1.01	cm^3/g
Surface area[31]	a_s	2304	m^2/g
Mean pore radius [27]	$\overline{r_0}$	1.5	mm
Specific heat of MOF-5[11]	$c_s(MOF-5)$	0.786	J/g/K
Specific heat of CO_2[28]	$c_s(CO_2)$	0.846	J/g/K
Specific heat of the MOF-5 with CO_2	c_s	815	J/kg/K
Thermal conductivity of CO_2[6]	λ_g	0.01617	W/m/K
Thermal conductivity of MOF-5[8]	λ_s	0.32	KW/m/K
Effective thermal conductivity	λ	0.0854	W/m/K
Conduction heat transfer coefficient	h(cond)	646.8	W/m2 K
Radiation heat transfer coefficient	h(rad)	2.8350	W/m2 K
Effective heat transfer coefficient	h	649.6350	W/m2 K
Boltzmann's constant	σ	5.78 x 10^{-12}	J/cm^2/s/K^4
Emissivity	$e_1 = e_2$	0.65	
Nusselt's number	Nu	2	
Temperature	T_0	296	K
Initial sorbate amount	M_0	0.45 x 10^{-3}	mole/g
Final sorbate amount	M_∞	0.53 x 10^{-3}	mole/g
Heat of adsorption	-ΔH	34.1	kJ/mol

Table C.3: Parameters Used in the New Analysis of CO_2 Adsorption on MOF-5

Parameter	Symbol	Value	Units
Diffusivity	D_0	8.87 x 10^{-13}	m^2/s
Activation Energy	Ea	7.61 x 10^3	J/mol
Gas constant	R	8.314	J/mol K
Adsorption	k_0	2.51 x 10^{-12}	Pa^{-1}
Pressure	p	101325	Pa
Total pore volume	V_p	1.01 x 10^{-3}	m^3/kg
Heat of adsorption	H	3.41 x 10^4	J/mol
Heat of adsorption	H	7.75 x 10^5	J/kg
Effective heat transfer coefficient	h	649	W/m^2 K
Effective thermal conductivity	λ	0.0854	W/m K
Effective heat capacity	c_p	815	J/kg K
Final CO_2 concentration	q_∞	2.1	mol/g
Final CO_2 concentration	q_∞	91.5842	kg of CO_2 per m^3 of MOF-5
Initial CO_2 concentration	q_0	0	kg of CO_2 per m^3 of MOF-5
Particle radius	r_0	2.50 x 10^{-5}	m
Density of porous MOF-5	ρ_e	130	kg/m^3
Density of solid MOF-5	ρ_0	750	kg/m^3
Temperature	T_0	295	K

Chapter D

SAMPLE DATA

Table D.1: $\Delta M_t/\Delta M_\infty$ for Stremming Expt

Time (s)	Crank	Isoth(Stremming)	Nonisoth(Stremming)
0	0.012	0.012	0.012
6.1224	0.0634	0.1176	0.2035
12.2449	0.089	0.166	0.2848
18.3673	0.1084	0.2031	0.346
24.4898	0.1245	0.2343	0.3968
30.6122	0.1387	0.2618	0.441
36.7347	0.1513	0.2867	0.4804
42.8571	0.1629	0.3095	0.5162
48.9796	0.1736	0.3307	0.549
55.102	0.1836	0.3507	0.5794
61.2245	0.1929	0.3695	0.6077
67.3469	0.2018	0.3874	0.6342
73.4694	0.2102	0.4044	0.659
79.5918	0.2182	0.4208	0.6824
85.7143	0.2259	0.4365	0.7044
91.8367	0.2333	0.4517	0.7251
97.9592	0.2404	0.4663	0.7446
104.0816	0.2472	0.4804	0.7629
110.2041	0.2538	0.4941	0.7801
116.3265	0.2603	0.5074	0.7963
122.449	0.2665	0.5203	0.8114
128.5714	0.2725	0.5329	0.8255
134.6939	0.2784	0.5451	0.8388
140.8163	0.2841	0.5571	0.8511

Table D.2: Effect of ΔH on Uptake and $\overline{\Delta T}$ –Stremming Expt

$\Delta H(J/mol)$								
	$4.19x10^4$		$4.19x10^5$		$83.8x10^5$		$167.6x10^5$	
Time (s)	Uptake	$\overline{\Delta T}$	Uptake	$\overline{\Delta T}$	Uptake	$\overline{\Delta T}$	Uptake	$\overline{\Delta T}$
0	0.012	0	0.012	0	0.012	0	0.012	0
6.1224	0.203	0.9712	0.1983	9.2251	0.1935	17.4959	0.1854	31.8002
12.2449	0.2841	1.2401	0.2776	11.8086	0.2712	22.4513	0.26	40.9817
18.3673	0.3452	1.3927	0.3375	13.2922	0.3298	25.3296	0.3165	46.4164
24.4898	0.3959	1.4854	0.3873	14.2081	0.3787	27.1352	0.3636	49.9141
30.6122	0.44	1.5399	0.4306	14.7636	0.4212	28.2595	0.4047	52.1803
36.7347	0.4794	1.5678	0.4693	15.0659	0.4592	28.9044	0.4415	53.5787
42.8571	0.5151	1.5757	0.5045	15.1789	0.4937	29.1908	0.475	54.3268
48.9796	0.5478	1.5682	0.5367	15.1447	0.5255	29.1978	0.5059	54.5668
55.102	0.5782	1.5483	0.5667	14.9929	0.555	28.981	0.5346	54.3986
61.2245	0.6064	1.5185	0.5946	14.7457	0.5826	28.5819	0.5615	53.8957
67.3469	0.6329	1.4806	0.6208	14.4206	0.6085	28.0329	0.5868	53.1153
73.4694	0.6577	1.4362	0.6454	14.0321	0.6328	27.3608	0.6106	52.1036
79.5918	0.6811	1.3867	0.6686	13.5928	0.6558	26.5883	0.6332	50.8995
85.7143	0.7031	1.3333	0.6905	13.1135	0.6776	25.7355	0.6546	49.5369
91.8367	0.7238	1.2771	0.7111	12.6041	0.6981	24.82	0.675	48.0456
97.9592	0.7433	1.2189	0.7306	12.0732	0.7176	23.8577	0.6943	46.4526
104.0816	0.7616	1.1597	0.749	11.5285	0.736	22.8629	0.7126	44.7819
110.2041	0.7788	1.1001	0.7663	10.9767	0.7534	21.8479	0.7301	43.0553
116.3265	0.795	1.0407	0.7827	10.4236	0.7698	20.8238	0.7466	41.2923
122.449	0.8101	0.9821	0.798	9.8742	0.7854	19.8	0.7623	39.5099
128.5714	0.8243	0.9247	0.8124	9.3326	0.8	18.7848	0.7772	37.7234

Effect of ΔH on Uptake and $\overline{\Delta T}$ –Stremming Expt... Cont'd

$\Delta H(J/mol)$								
	$4.19x10^4$		$4.19x10^5$		$83.8x10^5$		$167.6x10^5$	
Time (s)	Uptake	$\overline{\Delta T}$	Uptake	$\overline{\Delta T}$	Uptake	$\overline{\Delta T}$	Uptake	$\overline{\Delta T}$
159.1837	0.8823	0.6649	0.872	6.8418	0.861	14.0387	0.8405	29.1245
165.3061	0.8916	0.6194	0.8817	6.3992	0.871	13.1818	0.8511	27.5278
171.4286	0.9002	0.5763	0.8907	5.9773	0.8804	12.3607	0.861	25.9844
177.551	0.9082	0.5355	0.8991	5.5762	0.8892	11.5764	0.8704	24.4974
183.6735	0.9156	0.497	0.9068	5.1959	0.8974	10.8291	0.8792	23.0687
189.7959	0.9224	0.4608	0.9141	4.8363	0.905	10.119	0.8875	21.6998
195.9184	0.9288	0.4268	0.9208	4.4969	0.9121	9.4458	0.8952	20.3913
202.0408	0.9346	0.3949	0.927	4.1772	0.9187	8.8088	0.9025	19.1432
208.1633	0.94	0.365	0.9328	3.8767	0.9249	8.2073	0.9093	17.9553
214.2857	0.945	0.3372	0.9382	3.5948	0.9306	7.6402	0.9157	16.8266
220.4082	0.9496	0.3111	0.9431	3.3306	0.9359	7.1066	0.9216	15.7562
226.5306	0.9538	0.2869	0.9477	3.0835	0.9408	6.6052	0.9272	14.7425
232.6531	0.9577	0.2644	0.9519	2.8527	0.9454	6.1347	0.9324	13.784
238.7755	0.9613	0.2435	0.9558	2.6373	0.9496	5.6937	0.9372	12.879
244.898	0.9646	0.224	0.9594	2.4365	0.9536	5.281	0.9418	12.0254
251.0204	0.9676	0.2061	0.9627	2.2497	0.9572	4.8952	0.946	11.2215
257.1429	0.9704	0.1894	0.9658	2.0759	0.9606	4.5348	0.9499	10.4651
263.2653	0.9729	0.174	0.9686	1.9145	0.9637	4.1986	0.9536	9.7542
269.3878	0.9753	0.1597	0.9712	1.7646	0.9666	3.8852	0.957	9.0866
275.5102	0.9774	0.1466	0.9736	1.6257	0.9692	3.5934	0.9601	8.4604
281.6327	0.9794	0.1344	0.9758	1.4969	0.9717	3.3218	0.9631	7.8734
287.7551	0.9812	0.1232	0.9778	1.3777	0.974	3.0693	0.9658	7.3237

Table D.3: Effect of r_0 on Uptake and $\overline{\Delta T}$ –Stremming Expt, t = 10s

ro [t = linspace(0,10,50)]					
2.5 x 10^{-2}		2.5 x 10^{-3}		2.5 x 10^{-4}	
Uptake	$\overline{\Delta T}$	Uptake	$\overline{\Delta T}$	Uptake	$\overline{\Delta T}$
0.012	0	0.012	0	0.012	0
0.0123	0.0069	0.0379	0.2105	0.3611	1.4452
0.0125	0.0135	0.0535	0.2934	0.4992	1.6109
0.0128	0.0197	0.0654	0.3554	0.6002	1.5705
0.013	0.0256	0.0754	0.4064	0.681	1.4321
0.0133	0.0311	0.0842	0.4506	0.7474	1.2475
0.0136	0.0364	0.0922	0.4897	0.8019	1.0505
0.0139	0.0414	0.0994	0.5251	0.8461	0.8622
0.0142	0.0462	0.1062	0.5575	0.8814	0.6938
0.0145	0.0508	0.1126	0.5876	0.9093	0.5498
0.0148	0.0551	0.1185	0.6155	0.931	0.4304
0.0152	0.0593	0.1242	0.6418	0.9478	0.3335
0.0155	0.0632	0.1297	0.6665	0.9607	0.2563
0.0158	0.067	0.1349	0.6899	0.9706	0.1956
0.0161	0.0707	0.1399	0.7122	0.978	0.1484
0.0164	0.0741	0.1447	0.7334	0.9836	0.112
0.0168	0.0775	0.1493	0.7537	0.9878	0.0842
0.0171	0.0807	0.1538	0.7731	0.991	0.063
0.0174	0.0838	0.1582	0.7917	0.9934	0.047
0.0178	0.0868	0.1624	0.8096	0.9951	0.035
0.0181	0.0897	0.1666	0.8268	0.9964	0.0259
0.0184	0.0925	0.1706	0.8434	0.9974	0.0192

Effect of r_0 on Uptake and $\overline{\Delta T}$ –Stremming Expt, t = 10s... Cont'd

ro [t = linspace(0,10,50)]					
2.5 x 10^{-2}		2.5 x 10^{-3}		2.5 x 10^{-4}	
Uptake	$\overline{\Delta T}$	Uptake	$\overline{\Delta T}$	Uptake	$\overline{\Delta T}$
0.02	0.1053	0.1893	0.9187	0.9994	0.0041
0.0203	0.1077	0.1928	0.9324	0.9996	0.003
0.0206	0.1099	0.1963	0.9457	0.9997	0.0022
0.0209	0.1121	0.1997	0.9586	0.9998	0.0016
0.0213	0.1143	0.203	0.9712	0.9998	0.0012
0.0216	0.1164	0.2063	0.9835	0.9999	0.0008
0.0219	0.1185	0.2095	0.9954	0.9999	0.0006
0.0222	0.1205	0.2126	1.007	0.9999	0.0004
0.0225	0.1225	0.2157	1.0183	1	0.0003
0.0228	0.1244	0.2188	1.0294	1	0.0002
0.0231	0.1263	0.2218	1.0402	1	0.0002
0.0234	0.1282	0.2248	1.0507	1	0.0001
0.0236	0.13	0.2277	1.061	1	0.0001
0.0239	0.1318	0.2306	1.0711	1	0.0001
0.0242	0.1336	0.2335	1.0809	1	0.0001
0.0245	0.1353	0.2363	1.0905	1	0
0.0248	0.137	0.2391	1.0999	1	0
0.0251	0.1387	0.2418	1.1091	1	0
0.0253	0.1403	0.2445	1.1181	1	0
0.0256	0.142	0.2472	1.1269	1	0
0.0259	0.1436	0.2498	1.1356	1	0
0.0261	0.1451	0.2525	1.144	1	0

Table D.4: Effect of D_e on Uptake and $\overline{\Delta T}$ –Stremming Expt

De (m^2/s) [t = linspace(0,300,50)]					
$2.3x10^{-9}$		$2.3x10^{-8}$		$2.3x10^{-7}$	
Uptake	$\overline{\Delta T}$	Uptake	$\overline{\Delta T}$	Uptake	$\overline{\Delta T}$
0.012	0	0.012	0	0.012	0
0.203	0.9712	0.4494	4.4622	1.0338	15.1847
0.2841	1.2401	0.5976	4.9721	1.0865	9.8214
0.3452	1.3927	0.696	4.8538	1.0555	4.9704
0.3959	1.4854	0.768	4.4416	1.0277	2.2405
0.44	1.5399	0.8228	3.8895	1.0124	0.9469
0.4794	1.5678	0.865	3.296	1.0052	0.3842
0.5151	1.5757	0.8976	2.7239	1.0021	0.1515
0.5478	1.5682	0.9225	2.2077	1.0008	0.0586
0.5782	1.5483	0.9416	1.7621	1.0003	0.0223
0.6064	1.5185	0.9562	1.3894	1.0001	0.0084
0.6329	1.4806	0.9672	1.0846	1	0.0031
0.6577	1.4362	0.9755	0.8397	1	0.0011
0.6811	1.3867	0.9817	0.6456	1	0.0004
0.7031	1.3333	0.9864	0.4934	1	0.0001
0.7238	1.2771	0.9899	0.3752	1	0.0001
0.7433	1.2189	0.9925	0.284	1	0
0.7616	1.1597	0.9945	0.2142	1	0
0.7788	1.1001	0.9959	0.1609	1	0
0.795	1.0407	0.997	0.1206	1	0
0.8101	0.9821	0.9978	0.0901	1	0
0.8243	0.9247	0.9984	0.0671	1	0

Effect of D_e on Uptake and $\overline{\Delta T}$ –Stremming Expt... Cont'd

De (m^2/s) [t = linspace(0,300,50)]					
$2.3x10^{-9}$		$2.3x10^{-8}$		$2.3x10^{-7}$	
Uptake	$\overline{\Delta T}$	Uptake	$\overline{\Delta T}$	Uptake	$\overline{\Delta T}$
0.8823	0.6649	0.9997	0.015	1	0
0.8916	0.6194	0.9998	0.011	1	0
0.9002	0.5763	0.9998	0.0081	1	0
0.9082	0.5355	0.9999	0.006	1	0
0.9156	0.497	0.9999	0.0044	1	0
0.9224	0.4608	0.9999	0.0032	1	0
0.9288	0.4268	0.9999	0.0024	1	0
0.9346	0.3949	1	0.0017	1	0
0.94	0.365	1	0.0013	1	0
0.945	0.3372	1	0.0009	1	0
0.9496	0.3111	1	0.0007	1	0
0.9538	0.2869	1	0.0005	1	0
0.9577	0.2644	1	0.0004	1	0
0.9613	0.2435	1	0.0003	1	0
0.9646	0.224	1	0.0002	1	0
0.9676	0.2061	1	0.0001	1	0
0.9704	0.1894	1	0.0001	1	0
0.9729	0.174	1	0.0001	1	0
0.9753	0.1597	1	0.0001	1	0
0.9774	0.1466	1	0	1	0
0.9794	0.1344	1	0	1	0
0.9812	0.1232	1	0	1	0

Table D.5: $\Delta M_t/\Delta M_\infty$ and $\overline{\Delta T}$ CO2-MOF Adsorption

Time (s)	Crank	Iso(Stremming)	Non(Stremming)	$\overline{\Delta T}$
0	0.012	0.012	0.012	0
0.0002	0.0121	0.0276	0.2669	0.5751
0.0004	0.0122	0.039	0.3753	0.6892
0.0006	0.0123	0.0478	0.4575	0.7278
0.0008	0.0124	0.0552	0.5261	0.7277
0.001	0.0124	0.0617	0.5858	0.7036
0.0012	0.0125	0.0676	0.6387	0.6638
0.0014	0.0126	0.073	0.686	0.6141
0.0016	0.0127	0.0781	0.7284	0.5592
0.0018	0.0127	0.0828	0.7661	0.5023
0.002	0.0128	0.0873	0.7994	0.4463
0.0022	0.0129	0.0915	0.8287	0.3928
0.0024	0.013	0.0956	0.8543	0.3429
0.0027	0.0131	0.0995	0.8764	0.2974
0.0029	0.0131	0.1033	0.8955	0.2564
0.0031	0.0132	0.1069	0.9119	0.22
0.0033	0.0133	0.1104	0.9259	0.1879
0.0035	0.0134	0.1138	0.9379	0.1598
0.0037	0.0134	0.1172	0.948	0.1355
0.0039	0.0135	0.1204	0.9565	0.1145
0.0041	0.0136	0.1235	0.9637	0.0965
0.0043	0.0137	0.1266	0.9698	0.0811
0.0045	0.0138	0.1295	0.9749	0.0681
0.0047	0.0138	0.1325	0.9791	0.057

$\Delta M_t/\Delta M_\infty$ and $\overline{\Delta T}$ CO2-MOF Adsorption...Cont'd

Time (s)	Crank	Iso(Stremming)	Non(Stremming)	$\overline{\Delta T}$
0.0055	0.0141	0.1436	0.9902	0.0275
0.0057	0.0142	0.1462	0.9919	0.0228
0.0059	0.0143	0.1488	0.9933	0.0189
0.0061	0.0144	0.1513	0.9945	0.0157
0.0063	0.0144	0.1539	0.9955	0.013
0.0065	0.0145	0.1563	0.9963	0.0107
0.0067	0.0146	0.1588	0.9969	0.0089
0.0069	0.0147	0.1612	0.9975	0.0073
0.0071	0.0147	0.1635	0.9979	0.006
0.0073	0.0148	0.1658	0.9983	0.005
0.0076	0.0149	0.1681	0.9986	0.0041
0.0078	0.015	0.1704	0.9989	0.0034
0.008	0.015	0.1726	0.9991	0.0028
0.0082	0.0151	0.1749	0.9992	0.0023
0.0084	0.0152	0.177	0.9994	0.0019
0.0086	0.0152	0.1792	0.9995	0.0015
0.0088	0.0153	0.1813	0.9996	0.0013
0.009	0.0154	0.1834	0.9997	0.001
0.0092	0.0155	0.1855	0.9997	0.0008
0.0094	0.0155	0.1876	0.9998	0.0007
0.0096	0.0156	0.1896	0.9998	0.0006
0.0098	0.0157	0.1916	0.9998	0.0005
0.01	0.0158	0.1936	0.9999	0.0004

Table D.6: Effect of r_0 on Uptake and $\overline{\Delta T}$ – CO_2–MOF-5, t = 0.1s

ro [t = linspace(0,0.1,50)]					
25 x 10^{-6}		25 x 10^{-5}		25 x 10^{-4}	
Uptake	$\overline{\Delta T}$	Uptake	$\overline{\Delta T}$	Uptake	$\overline{\Delta T}$
0.012	0	0.012	0	0.012	0
0.4555	2.3012	0.0456	0.4187	0.0121	0.0193
0.642	2.0478	0.0645	0.58	0.0123	0.0366
0.7733	1.502	0.0789	0.6989	0.0126	0.0521
0.8625	0.9917	0.0911	0.7959	0.013	0.0661
0.9193	0.6149	0.1019	0.8789	0.0133	0.0788
0.9538	0.366	0.1116	0.9519	0.0138	0.0904
0.974	0.2119	0.1205	1.0174	0.0142	0.101
0.9856	0.1201	0.1288	1.0769	0.0147	0.1107
0.9921	0.067	0.1366	1.1314	0.0152	0.1198
0.9957	0.037	0.144	1.1819	0.0156	0.1282
0.9977	0.0202	0.1511	1.2289	0.0161	0.1361
0.9988	0.0109	0.1578	1.2729	0.0167	0.1434
0.9993	0.0059	0.1642	1.3142	0.0172	0.1504
0.9996	0.0031	0.1704	1.3531	0.0177	0.157
0.9998	0.0017	0.1764	1.3899	0.0182	0.1632
0.9999	0.0009	0.1822	1.4249	0.0187	0.1692
0.9999	0.0005	0.1878	1.4581	0.0192	0.1749
1	0.0002	0.1932	1.4897	0.0196	0.1803
1	0.0001	0.1985	1.5199	0.0201	0.1856
1	0.0001	0.2037	1.5488	0.0206	0.1907
1	0	0.2087	1.5764	0.0211	0.1956

Effect of r_0 on Uptake and $\overline{\Delta T}$ – CO_2–MOF-5, t = 0.1s... Cont'd

ro [t = linspace(0,0.1,50)]					
25 x 10^{-6}		25 x 10^{-5}		25 x 10^{-4}	
Uptake	$\overline{\Delta T}$	Uptake	$\overline{\Delta T}$	Uptake	$\overline{\Delta T}$
1	0	0.2322	1.6987	0.0233	0.218
1	0	0.2366	1.7204	0.0238	0.2222
1	0	0.241	1.7413	0.0242	0.2262
1	0	0.2453	1.7616	0.0246	0.2302
1	0	0.2495	1.7811	0.025	0.2341
1	0	0.2536	1.7999	0.0254	0.2379
1	0	0.2576	1.8181	0.0258	0.2417
1	0	0.2616	1.8357	0.0262	0.2454
1	0	0.2656	1.8526	0.0266	0.249
1	0	0.2695	1.8691	0.027	0.2525
1	0	0.2733	1.885	0.0274	0.256
1	0	0.2771	1.9004	0.0278	0.2595
1	0	0.2808	1.9153	0.0281	0.2629
1	0	0.2845	1.9297	0.0285	0.2662
1	0	0.2881	1.9437	0.0289	0.2695
1	0	0.2917	1.9572	0.0292	0.2728
1	0	0.2952	1.9704	0.0296	0.276
1	0	0.2987	1.9831	0.0299	0.2791
1	0	0.3022	1.9954	0.0303	0.2823
1	0	0.3056	2.0074	0.0306	0.2854
1	0	0.309	2.0189	0.0309	0.2884
1	0	0.3123	2.0302	0.0313	0.2914

Table D.7: Effect of D_e on Uptake and $\overline{\Delta T}$; CO2–MOF-5

De [t = linspace(0,0.01,50)]					
5.58 x 10^{-10}		5.58 x 10^{-9}		5.58 x 10^{-8}	
Uptake	$\overline{\Delta T}$	Uptake	$\overline{\Delta T}$	Uptake	$\overline{\Delta T}$
0.012	0	0.012	0	0.012	0
0.144	1.182	0.2665	5.7292	0.5105	23.0122
0.2036	1.549	0.3747	6.869	0.6909	20.4778
0.2494	1.7815	0.4569	7.2558	0.8092	15.0203
0.288	1.9443	0.5254	7.2577	0.8862	9.917
0.322	2.0626	0.5849	7.0207	0.934	6.1485
0.3528	2.1494	0.6378	6.627	0.9625	3.6603
0.3811	2.2123	0.6851	6.1346	0.9791	2.1186
0.4074	2.2565	0.7274	5.5884	0.9884	1.2012
0.4322	2.2852	0.7651	5.0236	0.9937	0.6704
0.4555	2.3012	0.7985	4.4657	0.9966	0.3696
0.4777	2.3064	0.8278	3.9328	0.9982	0.2017
0.4989	2.3022	0.8534	3.436	0.999	0.1092
0.5192	2.2899	0.8756	2.9817	0.9995	0.0587
0.5387	2.2706	0.8948	2.5724	0.9997	0.0313
0.5574	2.245	0.9113	2.2081	0.9999	0.0167
0.5755	2.2139	0.9253	1.8869	0.9999	0.0088
0.593	2.1781	0.9373	1.6063	1	0.0046
0.6099	2.1381	0.9475	1.3626	1	0.0024
0.6262	2.0945	0.9561	1.1524	1	0.0013
0.642	2.0478	0.9634	0.9718	1	0.0007
0.6572	1.9985	0.9695	0.8176	1	0.0003

Effect of D_e on Uptake and $\overline{\Delta T}$; CO2–MOF-5...Cont'd

De [t = linspace(0,0.01,50)]					
5.58 x 10^{-10}		5.58 x 10^{-9}		5.58 x 10^{-8}	
Uptake	$\overline{\Delta T}$	Uptake	$\overline{\Delta T}$	Uptake	$\overline{\Delta T}$
0.7263	1.7278	0.988	0.3342	1	0
0.7387	1.6712	0.9901	0.278	1	0
0.7507	1.6146	0.9918	0.231	1	0
0.7622	1.5581	0.9932	0.1917	1	0
0.7733	1.502	0.9944	0.1589	1	0
0.784	1.4465	0.9954	0.1315	1	0
0.7942	1.3916	0.9962	0.1088	1	0
0.8041	1.3376	0.9969	0.0899	1	0
0.8135	1.2845	0.9974	0.0742	1	0
0.8226	1.2326	0.9979	0.0612	1	0
0.8313	1.1818	0.9983	0.0504	1	0
0.8396	1.1323	0.9986	0.0415	1	0
0.8476	1.084	0.9988	0.0342	1	0
0.8552	1.0372	0.999	0.0281	1	0
0.8625	0.9917	0.9992	0.0231	1	0
0.8695	0.9476	0.9994	0.019	1	0
0.8761	0.905	0.9995	0.0156	1	0
0.8825	0.8638	0.9996	0.0128	1	0
0.8885	0.824	0.9996	0.0105	1	0
0.8943	0.7857	0.9997	0.0086	1	0
0.8998	0.7488	0.9998	0.007	1	0
0.9051	0.7132	0.9998	0.0057	1	0

Table D.8: Reduced CO_2 Concentration in MOF-5 Particle (η, τ)

Sample Reduced Concentration, U_1, Figure 5.20 at 10 s, and for N=10									
0	0	0	0	0	0	0	0	0	1.0016
0.1581	0.1693	0.2036	0.2639	0.3526	0.4694	0.6078	0.7546	0.8914	1
0.6236	0.6322	0.6575	0.6972	0.748	0.8053	0.8639	0.9186	0.965	1
0.8579	0.8613	0.8714	0.8871	0.9067	0.9285	0.9504	0.9706	0.9874	1
0.947	0.9483	0.9521	0.958	0.9654	0.9735	0.9817	0.9891	0.9954	1
0.9803	0.9807	0.9822	0.9844	0.9871	0.9901	0.9932	0.996	0.9983	1
0.9926	0.9928	0.9933	0.9941	0.9952	0.9963	0.9974	0.9985	0.9994	1
0.9973	0.9973	0.9975	0.9978	0.9982	0.9986	0.9991	0.9994	0.9998	1
0.9988	0.9989	0.9989	0.9991	0.9992	0.9994	0.9996	0.9998	0.9999	1
0.9996	0.9996	0.9996	0.9996	0.9997	0.9998	0.9998	0.9999	1	1

Table D.9: Reduced MOF-5 Particle Temperature (η, τ)

Reduced Temperature, U_2, Figure 5.21 at 10s, and for N=10									
1	1	1	1	1	1	1	1	1	1
1.0121	1.0121	1.0121	1.0121	1.012	1.012	1.012	1.012	1.012	1.012
1.0052	1.0052	1.0052	1.0052	1.0052	1.0052	1.0052	1.0052	1.0052	1.0052
1.002	1.002	1.002	1.002	1.002	1.002	1.002	1.0019	1.0019	1.0019
1.0007	1.0007	1.0007	1.0007	1.0007	1.0007	1.0007	1.0007	1.0007	1.0007
1.0003	1.0003	1.0003	1.0003	1.0003	1.0002	1.0002	1.0002	1.0002	1.0002
1.0001	1.0001	1.0001	1.0001	1.0001	1.0001	1.0001	1.0001	1.0001	1.0001
1	1	1	1	1	1	1	1	1	1
1	1	1	1	1	1	1	1	1	1
1	1	1	1	1	1	1	1	1	1

Table D.10: Reduced Temperature and CO_2 Concentration in MOF-5 Particle (τ)

Reduced Time	$U_1(\tau)$	$U_2(\tau)$	Temperature (K)	Diffusivity(m^2/s)
0	0.0102	1	295	8.17E-13
0.2041	0.1341	1.0173	300.1123	8.17E-13
0.4082	0.2107	1.0193	300.7077	1.72E-11
0.6122	0.2846	1.0188	300.5379	8.17E-13
0.8163	0.3622	1.0172	300.0806	8.17E-13
1.0204	0.4423	1.0153	299.5213	8.17E-13
1.2245	0.5202	1.0134	298.9467	8.17E-13
1.4286	0.5922	1.0115	298.3994	8.17E-13
1.6327	0.6563	1.0098	297.9004	8.17E-13
1.8367	0.7118	1.0083	297.4572	8.17E-13
2.0408	0.7593	1.007	297.0702	8.17E-13
2.2449	0.7993	1.0059	296.7368	8.17E-13
2.449	0.833	1.0049	296.4523	8.17E-13
2.6531	0.8611	1.0041	296.2112	8.17E-13
2.8571	0.8845	1.0034	296.0081	8.17E-13
3.0612	0.9039	1.0028	295.8379	8.17E-13
3.2653	0.9201	1.0024	295.6955	8.17E-13
3.4694	0.9334	1.002	295.5771	8.17E-13
3.6735	0.9446	1.0016	295.4779	8.17E-13
3.8776	0.9538	1.0013	295.3962	8.17E-13
4.0816	0.9616	1.0011	295.3275	8.17E-13
4.2857	0.968	1.0009	295.2712	8.17E-13
4.4898	0.9734	1.0008	295.2239	8.17E-13
4.6939	0.9779	1.0006	295.1852	8.17E-13

Reduced Temperature and CO_2 Concentration in MOF-5 Particle (τ)...*Cont'd*

Reduced Time	$U_1(\tau)$	$U_2(\tau)$	Temperature (K)	Diffusivity(m^2/s)
5.7143	0.9911	1.0002	295.0719	8.17E-13
5.9184	0.9926	1.0002	295.0595	8.17E-13
6.1224	0.9939	1.0002	295.0491	8.17E-13
6.3265	0.9949	1.0001	295.0407	8.17E-13
6.5306	0.9957	1.0001	295.0335	8.17E-13
6.7347	0.9964	1.0001	295.0277	8.17E-13
6.9388	0.997	1.0001	295.0228	8.17E-13
7.1429	0.9975	1.0001	295.0187	8.17E-13
7.3469	0.998	1.0001	295.0155	8.17E-13
7.551	0.9983	1	295.0128	8.17E-13
7.7551	0.9986	1	295.0106	8.17E-13
7.9592	0.9988	1	295.009	8.17E-13
8.1633	0.999	1	295.0077	8.17E-13
8.3673	0.9991	1	295.0066	8.17E-13
8.5714	0.9993	1	295.0055	8.17E-13
8.7755	0.9994	1	295.0047	8.17E-13
8.9796	0.9994	1	295.0041	8.17E-13
9.1837	0.9995	1	295.0036	8.17E-13
9.3878	0.9996	1	295.0031	8.17E-13
9.5918	0.9997	1	295.0025	8.17E-13
9.7959	0.9997	1	295.002	8.17E-13
10	0.9998	1	295.0016	8.17E-13